siRNA treated cells took on a relatively round shape with larger intercellular spaces (Fig. 5B).

The effect of CEACAM1 on cell aggregation of HepG2 cells

In the cell-aggregation assay, mock transfectants immediately aggregated and formed cell spheroids of 5–100 cells. CEACAM1-siRNA transfected cells formed smaller cell clusters, mostly of less than 10 cells (Fig. 6A). The percentage of single-free cells was 0.6±0.3% in mock transfectants, 5±1% in CEACAM1-siRNA#1 treated cells, and 4±1% in CEACAM1-siRNA#2-treated cells ($p<0.05$ and $p<0.05$ compared with mock transfectants) (Fig. 6B). When HepG2 cells in suspension culture were treated with hyaluronidase to prevent cell aggregation, cell proliferation was significantly decreased (control *vs.* hyaluronidase; 3.0±0.3, 1.5±0.5×10^5 cells/mL; $p<0.05$) (Fig. 6B).

Discussion

Our results showed that CEACAM1, which is generally considered to be a tumor suppressor (Hsieh et al., 1995; Kunath et al., 1995; Luo et al., 1999; Busch et al., 2002), exerts a dual effect on the proliferation potency of hepatoma cells. We found that the major four splice variants of CEACAM1 mRNA (CEACAM1-3L, 3S, 4L and 4S) were expressed in all hepatoma cell lines to varying degrees. However, as previously reported (Tanaka et al., 1997), our immunoblotting showed that CEACAM1 protein was not expressed in most of the hepatoma cells. Only HepG2 cells exhibited a protein band with molecular weight of approximately 110–130 kDa, which corresponds to CEACAM1-4L or CEACAM1-4S, in both monolayer and suspension culture. Because the difference in the molecular weight of CEACAM1-4L (long cytoplasmic domain) and CEACAM1-4S (short cytoplasmic domain) is only 8 kDa, it is difficult to distinguish these two isoforms even when extensive separation is performed by SDS-polyacrylamide gels (Houde et al., 2003). Nevertheless, we surmise that CEACAM1-S expression is unlikely, because the regulatory effect on epithelial cell proliferation is governed by the long cytoplasmic domain of CEACAM1-4L but not by CEACAM1-4S (Izzi et al., 1999). Immunofluorescence staining showed a strong localization of CEACAM at the cell–cell attachment area of HepG2 cells in monolayer culture, but not cells in suspension culture. Recently, Singer et al. reported that lateral immunostaining of CEACAM1 was only visible in highly polarized bladder epithelial cells permeabilized with Triton-X (Singer et al., 2000). HepG2 cells may become more polarized in monolayer culture than suspension culture, which is observed in many other epithelial types of cancer cells.

Our cell proliferation assay revealed that HepG2 cells exhibited a distinct biological feature compared with several other hepatoma cell lines, in terms of enhanced proliferation potential in suspension culture. To investigate the functional consequence of CEACAM1 expression on this unique proliferation potential, the effect of siRNA targeting of CEACAM1 on the growth rate of HepG2 cells was examined. When HepG2 cells were cultured in monolayer, inhibition of CEACAM1 expression by siRNA augmented the growth rate to approximately twice that of mock transfectants. When the same cells were cultured in suspension, however, the growth rate of CEACAM1-siRNA transfected cells was significantly decreased. In this setting, the ratio of apoptotic cells was not increased in CEACAM1-siRNA transfected cells, while the BrdU labeling index was reduced as compared with the cells transfected with control siRNA. These lines of evidence strongly indicate that CEACAM1 acts as a tumor suppressor in HepG2 cells in monolayer culture, whereas it promotes proliferation of cells in suspension culture. Because the ability of cancer cells to grow in suspension in vitro often correlates with the potential for tumorigenesis or metastasis in vivo (Rhim, 1983), our findings may indicate a novel effect of CEACAM1 in the progression of HCC. We are planning to conduct animal studies to further evaluate the clinical significance of our in vitro findings.

It has been generally accepted that normal epithelial cells require signals generated by cell-extracellular matrix interactions for cell survival, and fall into a form of apoptosis called anoikis in the absence of extracellular matrices. In contrast, many cancer cells of epithelial origin are anoikis resistant and can proliferate without matrix attachment, which is referred to as anchorage-independent growth. Although the exact mechanism of anchorage-independent growth has not been clarified, several studies have suggested that cell–cell attachment is involved in the survival and growth of cancer cells in the absence of cell-matrix interaction. Kantak et al. reported that oral squamous cell carcinoma cells require formation of E-cadherin-mediated cell aggregates to proliferate in suspension culture (Kantak and Kramer, 1998). Mueller et al. reported that colon cancer cells engineered to lack p21 or treated with hyaluronidase cannot form cell–cell contact and ceased proliferation in suspension culture (Mueller et al., 2000). Lawlor et al. reported that cell aggregation was required for the anchorage-independent growth of Ewing tumor cells, and that cyclin D_1 was not induced until cell spheroids had formed in suspension culture (Lawlor et al., 2002). More recently, Shen et al. reported that cell–cell attachment is necessary for anchorage-independent growth of squamous cell carcinoma, because cell–cell contact specifically activates epidermal growth factor receptor which in turn triggers the extracellular signal-regulated kinase (ERK) and mitogen-activated protein kinase (MAPK) signaling modules (Shen and Kramer, 2004). In this study, we found that inhibition of CEACAM1 expression in HepG2 cells in suspension culture not only resulted in a reduced growth rate but also decreased the cell–cell attachment rate. Moreover, hyaluronidase treatment resulted in significant blockade of proliferation of HepG2 cells in suspension culture, indicating that cell–cell attachment is required for anchorage-independent growth. Considering these facts together, cell–cell attachment via homophilic interaction of CEACAM1 (Obrink, 1997; Brummer et al., 2001) might be essential for the enhanced anchorage-independent growth in HepG2 cells.

To date, there have been only a few studies investigating the role of CEACAM1 in anchorage-independent growth of cancer cells. Hsieh et al. reported that prostatic cancer cells transfected with CEACAM1 showed reduced anchorage-independent growth

and less tumorigenicity in vivo (Hsieh et al., 1995). Laurie et al. reported that enforced expression of CEACAM1-4L in a rat hepatoma cell line resulted in smaller cell aggregate size in anchorage-independent growth conditions, and delayed cell-cycle progression through the G1-S phase (Laurie et al., 2005). Although these two reports seem to contradict what we observed in our study, it should be noted that the level of indigenous CEACAM1 expression was low in the cell lines they used, in contrast to HepG2 cells which have strong CEACAM1 expression. We surmise that although exogenously induced CEACAM1 may act as a complete tumor suppressor in cancer cells that intrinsically lack CEACAM1, in some cancer cells such as HepG2 with strong CEACAM expression, CEACAM1 may play an important role in enhancing anchorage-independent growth by potentiating cell–cell attachment between neighboring cancer cells.

Conclusion

In the present study, we demonstrated that CEACAM1 is lost in most human hepatoma cells except HepG2 cells, which showed an enhanced growth rate in anchorage-independent growth conditions. CEACAM1 acted as a tumor suppressor for HepG2 cells in monolayer culture, but promoted growth in the absence of cell-matrix interaction by potentiating cell–cell attachment. Although it is not clear whether our findings could be applicable to other types of cancer cells, we suggest that further investigation of the functional consequence of CEACAM1 expression in cancer cells may help to better understand the metastatic behavior of HCC.

Acknowledgment

This work was supported in part by the Grant-in-Aid for Scientific Research #18591504 (T.W. and Y.S.) from the Ministry of Education, Culture, Sports, Science and Technology of Japan.

References

Bamberger, A.M., Riethdorf, L., Nollau, P., Naumann, M., Erdmann, I., Gotze, J., Brummer, J., Schulte, H.M., Wagener, C., Loning, T., 1998. Dysregulated expression of CD66a (BGP, C-CAM), an adhesion molecule of the CEA family, in endometrial cancer. American Journal of Pathology 152, 1401–1406.

Brummer, J., Neumaier, M., Gopfert, C., Wagener, C., 1995. Association of pp60c-src with biliary glycoprotein (CD66a), an adhesion molecule of the carcinoembryonic antigen family downregulated in colorectal carcinomas. Oncogene 11, 1649–1655.

Brummer, J., Ebrahimnejad, A., Flayeh, R., Schumacher, U., Loning, T., Bamberger, A.M., Wagener, C., 2001. Cis interaction of the cell adhesion molecule CEACAM1 with integrin beta(3). American Journal of Pathology 159, 537–546.

Busch, C., Hanssen, T.A., Wagener, C., OBrink, B., 2002. Downregulation of CEACAM1 in human prostate cancer: correlation with loss of cell polarity, increased proliferation rate, and Gleason grade 3 to 4 transition. Human Pathology 33, 290–298.

Cruz, P.V., Wakai, T., Shirai, Y., Yokoyama, N., Hatakeyama, K., 2005. Loss of carcinoembryonic antigen-related cell adhesion molecule 1 expression is an adverse prognostic factor in hepatocellular carcinoma. Cancer 104, 354–360.

Ebrahimnejad, A., Streichert, T., Nollau, P., Horst, A.K., Wagener, C., Bamberger, A.M., Brummer, J., 2004. CEACAM1 enhances invasion and migration of melanocytic and melanoma cells. American Journal of Pathology 165, 1781–1787.

Houde, C., Roy, S., Leung, N., Nicholson, D.W., Beauchemin, N., 2003. The cell adhesion molecule CEACAM1-L is a substrate of caspase-3-mediated cleavage in apoptotic mouse intestinal cells. Journal of Biological Chemistry 278, 16929–16935.

Hsieh, J.T., Luo, W., Song, W., Wang, Y., Kleinerman, D.I., Van, N.T., Lin, S.H., 1995. Tumor suppressive role of an androgenregulated epithelial cell adhesion molecule (C-CAM) in prostate carcinoma cell revealed by sense and antisense approaches. Cancer Research 55, 190–197.

Izzi, L., Turbide, C., Houde, C., Kunath, T., Beauchemin, N., 1999. cis-Determinants in the cytoplasmic domain of CEACAM1 responsible for its tumor inhibitory function. Oncogene 18, 5563–55672.

Kantak, S.S., Kramer, R.H., 1998. E-cadherin regulates anchorage-independent growth and survival in oral squamous cell carcinoma cells. Journal of Biological Chemistry 273, 16953–16961.

Kinugasa, T., Kuroki, M., Takeo, H., Matsuo, Y., Ohshima, K., Yamashita, Y., Shirakusa, T., Matsuoka, Y., 1998. Expression of four CEA family antigens (CEA, NCA, BGP and CGM2) in normal and cancerous gastric epithelial cells: up-regulation of BGP and CGM2 in carcinomas. International Journal of Cancer 76, 148–153.

Kleinerman, D.I., Troncoso, P., Lin, S.H., Pisters, L.L., Sherwood, E.R., Brooks, T., von Eschenbach, A.C., Hsieh, J.T., 1995. Consistent expression of an epithelial cell adhesion molecule (C-CAM) during human prostate development and loss of expression in prostate cancer: implication as a tumor suppressor. Cancer Research 55, 1215–1220.

Kleinerman, D.I., Dinney, C.P., Zhang, W.W., Lin, S.H., Van, N.T., Hsieh, J.T., 1996. Suppression of human bladder cancer growth by increased expression of C-CAM1 gene in an orthotopicmodel. Cancer Research 56, 3431–3435.

Kunath, T., Ordonez-Garcia, C., Turbide, C., Beauchemin, N., 1995. Inhibition of colonic tumor cell growth by biliary glycoprotein. Oncogene 11, 2375–2382.

Laack, E., Nikbakht, H., Peters, A., Kugler, C., Jasiewicz, Y., Edler, L., Brummer, J., Schumacher, U., Hossfeld, D.K., 2002. Expression of CEACAM1 in adenocarcinoma of the lung: a factor of independent prognostic significance. Journal of Clinical Oncology 20, 4279–4284.

Laurie, N.A., Comegys, M.M., Carreiro, M.P., Brown, J.F., Flanagan, D.L., Brilliant, K.E., Hixson, D.C., 2005. Carcinoembryonic antigen-related cell adhesion molecule 1a-4L suppression of rat hepatocellular carcinomas. Cancer Research 65, 11010–11017.

Lawlor, E.R., Scheel, C., Irving, J., Sorensen, P.H., 2002. Anchorage-independent multi-cellular spheroids as an in vitro model of growth signaling in Ewing tumors. Oncogene 21, 307–318.

Liu, W., Wei, W., Winer, D., Bamberger, A.M., Bamberger, C., Wagener, C., Ezzat, S., Asa, S.L., October 23, 2006. CEACAM1 impedes thyroid cancer growth but promotes invasiveness: a putative mechanism for early metastases. Oncogene advance online publication.

Luo, W., Tapolsky, M., Earley, K., Wood, C.G., Wilson, D.R., Logothetis, C.J., Lin, S.H., 1999. Tumor-suppressive activity of CD66a in prostate cancer. Cancer Gene Therapy 6, 313–321.

McCaffrey, T.A., Fu, C., Du, B., Eksinar, S., Kent, K.C., Bush Jr., H., Kreiger, K., Rosengart, T., Cybulsky, M.I., Silverman, E.S., Collins, T., 2000. High-level expression of Egr-1 and Egr-1-inducible genes in mouse and human atherosclerosis. Journal of Clinical Investigation 105, 653–662.

Mueller, S., Cadenas, E., Schonthal, A.H., 2000. $p21^{WAF1}$ regulates anchorage-independent growth of HCT116 colon carcinoma cells via E-cadherin expression. Cancer Research 60, 156–163.

Naito, Y., Yamada, T., Ui-Tei, K., Morishita, S., Saigo, K., 2004. siDirect: highly effective, target-specific siRNA design software for mammalian RNA interference. Nucleic Acids Research 32, W124–W129.

Neumaier, M., Paululat, S., Chan, A., Matthaes, P., Wagener, C., 1993. Biliary glycoprotein, a potential human cell adhesion molecule, is down-regulated in colorectal carcinomas. Proceedings of the National Academy of Sciences of the United States of America 90, 10744–10748.

Obrink, B., 1997. CEA adhesion molecules: multifunctional proteins with signal-regulatory properties. Current Opinion in Cell Biology 9, 616–626.

Rhim, J.S., 1983. Cell aggregation assay: a rapid means of evaluating and selecting in vitro transformed cells. Cancer Detection and Prevention 6, 381–388.

Riethdorf, L., Lisboa, B.W., Henkel, U., Naumann, M., Wagener, C., Loning, T., 1997. Differential expression of CD66a (BGP), a cell adhesion molecule of the carcinoembryonic antigen family, in benign, premalignant, and malignant

lesions of the human mammary gland. Journal of Histochemistry and Cytochemistry 45, 957–963.

Shen, X., Kramer, R.H., 2004. Adhesion-mediated squamous cell carcinoma survival through ligand-independent activation of epidermal growth factor receptor. American Journal of Pathology 165, 1315–1329.

Sienel, W., Dango, S., Woelfle, U., Morresi-Hauf, A., Wagener, C., Brummer, J., Mutschler, W., Passlick, B., Pantel, K., 2003. Elevated expression of carcinoembryonic antigen-related cell adhesion molecule 1 promotes progression of non-small cell lung cancer. Clinical Cancer Research 9, 2260–2266.

Singer, B.B., Scheffrahn, I., Obrink, B., 2000. The tumor growth-inhibiting cell adhesion molecule CEACAM1 (C-CAM) is differently expressed in proliferating and quiescent epithelial cells and regulates cell proliferation. Cancer Research 60, 1236–1244.

Takahashi, H., Okai, Y., Paxton, R.J., Hefta, L.J., Shively, J.E., 1993. Differential regulation of carcinoembryonic antigen and biliary glycoprotein by γ-interferon. Cancer Research 53, 1612–1619.

Tanaka, K., Hinoda, Y., Takahashi, H., Sakamoto, H., Nakajima, Y., Imai, K., 1997. Decreased expression of biliary glycoprotein in hepatocellular carcinomas. International Journal of Cancer 74, 15–19.

Thies, A., Moll, I., Berger, J., Wagener, C., Brummer, J., Schulze, H.J., Brunner, G., Schumacher, U., 2002. CEACAM1 expression in cutaneous malignant melanoma predicts the development of metastatic disease. Journal of Clinical Oncology 20, 2530–2536.

Yano, H., Maruiwa, M., Murakami, T., Fukuda, K., Ito, Y., Sugihara, S., Kojiro, M., 1988. A new human pleomorphic hepatocellular carcinoma cell line, KYN-2. Acta pathologica Japonica 38, 953–966.

Zhang, X., Emerald, B.S., Mukhina, S., Mohankumar, K.M., Kraemer, A., Yap, A.S., Gluckman, P.D., Lee, K.O., Lobie, P.E., 2006. HOXA1 is required for E-cadherin-dependent anchorage-independent survival of human mammary carcinoma cells. Journal of Biological Chemistry 281, 6471–6481.

The cost-effectiveness of the new protocol reflecting rapid virologic response to peginterferon α-2b and ribavirin for chronic hepatitis C

Junichiro Nakamura[a], Kuriko Kobayashi[a], Shin-ichi Toyabe[a], Yutaka Aoyagi[b] and Kouhei Akazawa[a]

Objective **Recent studies have reported the effectiveness of shorter courses of treatment with peginterferon α-2b plus ribavirin for patients with chronic hepatitis C, who achieved a rapid virologic response (RVR), defined as undetectable hepatitis C virus (HCV-) RNA at week 4. The aim of this study was to evaluate the cost-effectiveness of the new protocol for treatment, from the perspective of RVR.**

Methods **A cost-effectiveness analysis based on the rate of sustained virologic response was performed. A Markov cohort model of hepatitis C was constructed to demonstrate the clinical states on the basis of the assigned transition probabilities over 30 years. The treatment strategies were classified into five subgroups taking into consideration the viral genotypes, viral load, and RVR. The lifetime costs and quality-adjusted life years (QALYs) were compared between the new and standard protocols for treatment.**

Results **Genotype 1-infected patients in the new protocol for treatment compared with the standard one could prolong QALYs by 0.33 and reduce lifetime cost by € 5993. Genotype 2 or 3-infected patients in the new protocol for treatment compared with the standard one could prolong QALYs by 0.02 and reduce lifetime cost by €2851.**

Conclusion **Treatment strategies that consider viral load and RVR for patients with a low viral load infected with genotype 1 and those infected with genotype 2 or 3 are more cost-effective compared with the standard protocol for treatment. *Eur J Gastroenterol Hepatol* 19:733–739**

European Journal of Gastroenterology & Hepatology 2007, 19:733–739

Keywords: cost effectiveness, peginterferon α-2b, rapid virologic response, ribavirin

Divisions of [a]Information Science and Biostatistics and [b]Gastroenterology and Hepatology, Niigata University Graduate School of Medical and Dental Sciences, Niigata, Japan

Correspondence to Mr Junichiro Nakamura, MD, Division of Information Science and Biostatistics, Niigata University Graduate School, 1-754, Asahimachi-dori, Niigata 951-8520, Japan
Tel: +81 25 227 2472; fax: +81 25 227 0850;
e-mail: ichirojn@med.niigata-u.ac.jp

Received 12 March 2007 Accepted 15 May 2007

Introduction

Hepatitis C infection is the leading cause of hepatocellular carcinoma (HCC), and 180 million people are estimated to be infected with hepatitis C worldwide [1]. About a third of the HCC cases are caused by a hepatitis C infection. An increasing number of incidences of HCC over the past two decades have been reported in the United States [2]. The average annual age-adjusted incidence of HCC increased from 1.3/100 000 for the period from 1981 to 1983 to 3.0/100 000 for the period from 1996 to 1998 in the United States, and similar trends were seen in Europe [3,4].

Currently, to eradicate the hepatitis C virus (HCV) from infected patients, the only treatment option is antiviral therapy. Patients achieving a sustained virologic response (SVR) with the antiviral therapy can maintain viral control during their lifetimes and have very low incidences of HCC. In the 1990s, interferon monotherapy was the primary treatment. Recently, peginterferon in combination with ribavirin has been found to be more effective than interferon alone or interferon in combination with ribavirin, especially for genotype 1-infected patients [5,6]. The SVR rate of 42% reported by Manns *et al.* [5] was significantly higher in genotype 1-infected patients treated with peginterferon α-2b plus ribavirin than that of 33% in those treated with interferon α-2b plus ribavirin. The National Institute of Health Consensus Development Conference and the American Association for the Study of Liver Disease recommended that untreated patients should be treated with peginterferon in combination with ribavirin (1000–1200 mg) for 48 weeks in genotype 1 cases, and in combination with ribavirin (800 mg) for 24 weeks in genotype 2 or 3 cases, without contradictions [2,7].

From an economic perspective, the combination therapy of peginterferon plus ribavirin is associated with an increase in treatment cost. Conversely, the lifetime cost for treatment can be reduced by the combination therapy, as patients achieving SVR need not be treated any further. Several studies have reported that the combination

0954-691X

therapy increased the lifetime cost but prolonged the quality-adjusted life years (QALYs), and have concluded that it was cost-effective [8–10]. More recently, the results of the cost-effectiveness analyses that considered the effects of the virologic response in the early weeks (at week 12) were also reported [11,12]. In these studies, the assessment at week 12 for genotype 1 resulted in the reduction of the lifetime cost by 21.2%; the HCV core-antigen test at week 12 for genotype 1 was associated with a reduction in cost per successfully treated patient of 9.7%. Furthermore, other studies have reported the evaluation at a much earlier period (at week 4) of treatment [13,14].

A total of six major genotypes have been reported; however, genotypes 1, 2, and 3 are the most common worldwide. For example, genotype 1 accounts for 75.3% of all cases in the United States, followed by genotypes 2 (16.3%) and 3 (8.5%) [15]. For a cost-effectiveness analysis, it is necessary to take into account the differences of the viral responses to antiviral therapy among the different viral genotypes. Our study was, therefore, performed taking the viral genotypes into consideration.

Our study is a cost-effectiveness analysis to systematically evaluate the rapid virologic response (RVR) at week 4 in both genotype 1 with a low viral load and in genotypes 2 and 3. The aim of this study was to assess the cost-effectiveness of the new protocol for the treatment of hepatitis C, after factoring in the RVR to peginterferon α-2b and ribavirin in genotypes 1, 2, and 3.

Materials and methods

Model

A Markov cohort model of chronic hepatitis C disease progression was constructed to evaluate the cost-effectiveness of different treatment strategies (Fig. 1). In the Markov model, the cohort begins with an initial health state (chronic hepatitis C); the patients in the cohort could remain in the same state or move to the next state, according to the transition probabilities at each cycle [16,17]. When the Markov cohort analysis is terminated at end point, the total number of patient-cycles for each state is divided by the size of the original cohort; this yields the expected time that each individual will spend in each state. Life expectancy (LE) is the sum of these expected values, and lifetime cost can be calculated in the same way. Figure 1 demonstrates our model. Five Markov states are described in it, and circles and rectangles show transient states and outcomes of death, respectively.

Treatment assumptions

Chronic hepatitis C was defined as a serologic positive for HCV, HCV-RNA-positive, and elevated aminotransferase.

Fig. 1

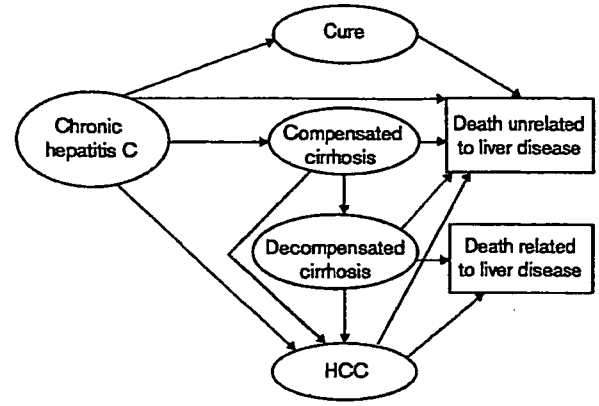

Overview of the Markov cohort model of hepatitis C. Five Markov states were described in this model. The circles and rectangles show the transient states and outcomes of death, respectively. HCC, hepatocellular carcinoma.

Decompensated cirrhosis was determined by the presence of ascites, variceal hemorrhage, or encephalopathy. The antiviral therapy considered in this study was peginterferon α-2b, in combination with ribavirin; patients with hepatitis C initially received this combination. The average dose of peginterferon α-2b was assumed to be 100 μg/week. The dose of ribavirin was determined by the genotypes; the average doses of ribavirin for genotype 1 patients and for genotypes 2 and 3 were assumed to be 1000 and 800 mg/day, respectively. All the patients required hospitalization and underwent liver biopsies.Their serum levels of HCV-RNA were quantified by the real-time polymerase-chain-reaction (RT-PCR) assay at the onset of treatment. SVR was defined as being serum HCV-RNA negative, both at the end of treatment, and after 24 weeks of follow-up. In view of the viral response data reported in several studies, we proposed a new protocol for the treatment of chronic hepatitis C, which was classified into five subgroups [5,13,14]. Table 1 demonstrates our strategies, and the following assumptions that were made in them: the patients belonging to subgroups A and C discontinued treatment when they had detectable HCV-RNA at week 24, as a low likelihood of SVR was reported with an additional 24 weeks of treatment in these cases. The patients who relapsed after treatment or discontinued treatment were not retreated; they were assumed to have progressed to later stages, similar to untreated patients and received no benefit from the combination therapy.

Assumption in the model

The Markov cohort analysis was performed over the patient's lifetime (up to 30 years in this model). The simulations began with a hypothetical cohort of patients defined as being 45 years old, male, with chronic hepatitis C, and without cirrhosis or HCC.

Table 1 Treatment strategies considering viral genotypes, viral load, and viral response at week 4

	Genotype	Viral load	RVR (%, 95% CI)	Treatment duration (weeks)	SVR % (95% CI)	Reference
New protocol						
Subgroup A	1	High		48	37 (27–47)	[5]
Subgroup B	1	Low	Yes (47, 40–53)	24	89 (83–95)	[13]
Subgroup C	1	Low	No (53, 37–60)	48	64 (45–83)	[5,13]
(weighted average of subgroup B and C)[a]	1	Low			75 (63–88)	
Subgroup D	2 or 3	[b]	Yes (63, 57–69)	12	85 (79–91)	[14]
Subgroup E	2 or 3	[b]	No (37, 31–43)	24	60 (51–69)	[14]
(weighted average of subgroup D and E)[a]	2 or 3				78 (68–83)	
Standard protocol	1	[b]		48	48 (39–56)	[5]
	1	Low		48	71 (57–85)	[5,13]
	2 or 3	[b]		24	76 (66–86)	[14]

The results of the PCR testing at week 4 determined the treatment durations for patients infected with genotype 1 with a low viral load and those infected with genotype 2 or 3 in the new protocol. The durations were 12, 24, and 48 weeks.
CI, confidence interval; RVR, rapid virologic response (HCV-RNA negative at week 4); SVR, sustained virologic response.
[a]The weighted average using the rate of RVR.
[b]Viral load not considered.

Parameters in the model

The annual transition probabilities of progression to subsequent states were mainly taken from the literature. The probability of death for patients with HCC was obtained from the data on 1070 patients who were diagnosed with HCC at 31 hospitals in Japan [18–30] (Table 2). The literature was searched using Medline for similar studies published up to 2006; the following MeSH terms and their combinations were used for searching: hepatitis C, chronic, fibrosis, carcinoma, hepatocellular, and follow-up studies. The rates of RVR, SVR, and discontinuation used in our model were based on three clinical trials [5,13,14] (Table 1). The data of subgroups B and C were derived from the study by Zeuzem *et al.* [13], in which 235 genotype 1-infected patients with a low viral load (HCV-RNA $\leq$ 600 000 IU/ml) had been included. For subgroup D and E, the trial, which included 283 patients, was reported by Mangia *et al.*, of whom 70 patients were assigned to a 24-week regimen, and the other 213 patients to a variable regimen (12 or 24 weeks of treatment, depending on whether or not they achieve RVR) [14]. The estimated costs of patients who discontinued treatment were incorporated into our model by analyzing these three trials. The estimated annual cost for each state included only direct healthcare costs. Inpatient costs were derived from the actual data on the patients with decompensated cirrhosis and HCC. The outpatient costs included costs for hospital visits, laboratory tests, ultrasonography, radiography, and medical procedures, which were needed for the chronic hepatitis C-related states. All the costs were converted into Euros using 2006 exchange rates reported by the Organization for Economic Cooperation and Development (OECD) [31] (Table 3). The rates of ascites, variceal hemorrhage, and encephalopathy in the decompensated state were taken from the two prospective studies, and they were assumed to be 76.0, 18.5, and 5.5%, respectively [32,33]. The estimates of the values, which reflected the quality of life associated with the various states relating to chronic hepatitis C and combination therapy, were assigned to calculate QALYs. The values of health-related quality of life (HRQOL) varying from 0 (death) to 1 (perfect health) were taken from previously published studies [34] (Table 2). The age-specific death rates for the general population were also incorporated, and they were estimated by the abridged life table for Japan in 2004 [30].

Table 2 Transition probabilities and health related QOL in hepatitis C-related states estimated by published and unpublished sources

Transition probabilities	Baseline	95% CI	Reference
Chronic hepatitis			
To compensated cirrhosis	0.065	0.030–0.100	[18,19]
To HCC	0.016	0.005–0.027	[19–22]
Compensated cirrhosis			
To decompensated cirrhosis	0.085	0.025–0.061	[23,24]
To HCC	0.083	0.064–0.102	[22,24–29]
Decompensated cirrhosis			
To HCC	0.083	0.064–0.102	[22,24–29]
To death	0.129	0.090–0.177	[23]
HCC			
To death	0.200	0.176–0.224	*

Health-related QOL	QOL value	Reference
Chronic hepatitis	0.72	[30]
Compensated cirrhosis	0.55	[30]
Decompensated cirrhosis	0.45	[30]
HCC	0.45	[30]
Combination therapy	0.66	[30]
Post SVR	0.82	[30]

Health-related QOL reflected each health state between 0 (death) and 1 (perfect health).
CI, 95% confidence interval; HCC, hepatocellular carcinoma; QOL, quality of life; SVR, sustained virologic response.
*Unpublished sources in which 1070 patients diagnosed with HCC in 31 hospitals affiliated with the Niigata Liver Disease Study Group were followed up from 1993 to 2003.

Cost-effectiveness analysis

Lifetime cost, life expectancies (LEs) and QALYs were all calculated to evaluate the cost-effectiveness during

Table 3 Cost parameters based on the actual data, and model assumption

	Outpatient	Inpatient	Total
Annual cost (€)			
Chronic hepatitis	1289		1289
Compensated cirrhosis	1407		1407
Decompensated cirrhosis[a]		10687	12634
Ascites (76.0%)	(1595)[b]		
Variceal bleeding (18.5%)	(1995)[b]		
Encephalopathy (5.5%)	(6645)[b]		
Weighted average[c]	1947		
HCC	2991	11563	14554
Unit cost for combination therapy (€)			
Peginterferon α-2b (100 μg)		215	
Ribavirin (1 capsule at 200 mg)		5.59	
Cost of hospitalization except for drug cost		5102	

HCC, hepatocellular carcinoma.
[a]Decompensated cirrhosis was assumed to be with ascites, variceal bleeding, and encephalopathy.
[b]Prices in parentheses showed unit cost of the state.
[c]The weighted average was calculated using the rates of ascites, variceal bleeding, and encephalopathy.

30 years of follow-up. These measures in the cost-effectiveness analysis were compared between the new and standard protocols for treatment.

First, a base-case analysis was performed by incorporating the baseline parameters, which are shown in Tables 1 to 3, into the model. Next, a one-way sensitive analysis was performed by varying the parameters that might affect the lifetime cost, LEs, and QALYs. Such parameters as treatment effectiveness (i.e. SVR), rates of RVR, and transition probabilities varied, when respective 95% confidence intervals were applied. The prices of peginterferon α-2b and ribavirin varied by ± 50%. All the costs and benefits were discounted at a rate of 3%/year on the basis of international recommendations [35].

The analyses were performed using the TreeAge Pro 2006 software program (TreeAge Software, Williamstown, Massachusetts, USA). This study was approved by the ethics committees of Niigata Medical and Dental University Hospital.

Results

Base-case results in the Markov model

Table 4 presents the base-case results and the cost-effectiveness analysis in the model. The 10-year cumulative risk of progression to cirrhosis in hepatitis C patients without treatment was estimated to be 45.1% in our model, which is comparable with the 10-year risk of 47.4% reported by a Japanese research group [36]. Each strategy in the new protocol demonstrated the 10-year risk of cirrhosis and HCC to be 4.9–28.0% and 2.9–15.0%, respectively.

Base-case results in the cost-effectiveness analysis

As shown in Table 4, the combination therapy demonstrated extensive LEs of 15.90–18.20 years and QALYs of 11.36–14.54 compared with no treatment. According to the weighted average of the results of subgroups B and C, the genotype 1-infected patients with a low viral load in the new protocol for treatment gained the most prolonged QALYs and a more reduced lifetime cost compared with the same type of patients in the standard protocol. The weighted average of subgroup D and E (patients infected with genotype 2 or 3 in the new protocol for treatment) showed almost equivalent LEs and QALYs; however, they experienced a reduction in lifetime cost compared with the same type of patients in the standard protocol. The lifetime costs for patients infected with genotype 1, with a low viral load, and that for those infected with genotype 2 or 3 in the new protocol for treatment were calculated to be €38606 (saving 13.4% of the lifetime cost in the standard protocol) and €31154 (saving 8.4% of the lifetime cost in the standard protocol), respectively (Table 4).

Sensitivity analysis

Table 5 presents the probable ranges of the cost-effectiveness measures, which were determined by the result of a one-way sensitivity analysis; each measure was then compared between the new and standard protocols for treatment. In the one-way sensitivity analyses, the new protocol for treatment indicated that QALYs were prolonged by 0.22–1.07 in genotype 1 with a low viral load and by 0.02–0.44 in genotype 2 or 3, respectively, compared with similar groups of patients in the standard protocol. The QALYs in genotype 1 with a low viral load were shortened, however, when the patients in the new protocol achieved the lower limit of the SVR. Similarly, the QALYs in genotype 2 or 3 were shortened when the patients in the new protocol achieved the lower limits of not only SVR, but also RVR. As for the lifetime costs, all the results of the one-way sensitivity analysis indicated that the new protocol for treatment reduced lifetime costs by €2169–9765 in genotype 1 with a low viral load and by €109–5517 in genotype 2 or 3, respectively, compared with the standard protocol. The new protocol for treatment would, therefore, be the dominant strategy of the two, although the QALYs cannot be prolonged when it achieves the lower limit of the SVR or RVR.

Discussion

In our cost-effectiveness analysis, the new protocol that reflected RVR to the combination therapy for chronic hepatitis C was superior in terms of effectiveness and lifetime cost, compared with the standard protocol. In other words, it was referred to as being 'dominant' over the standard protocol for treatment.

Two sophisticated clinical trial groups reported the effectiveness of shorter courses of treatment for patients with RVR. The rates of adverse events that led to the discontinuation of treatment or to dose reduction of

Table 4 Results of base-case analysis in the Markov model over the cohorts' lifetime up to 30 years and the cost-effectiveness analysis

	New protocol							Standard protocol			No treatment
Subgroup	A	B	C	(Weighted average of subgroup B and C)[a]	D	E	(Weighted average of subgroup D and E)[a]				
Genotype	1	1	1	1	2 or 3	2 or 3	2 or 3	1	1	2 or 3	
Viral load	High	Low	Low	Low	[b]	[b]	[b]	[b]	Low	[b]	
		RVR+	RVR−		RVR+	RVR−					
Treatment duration (weeks)	48	24	48	24 or 48	12	24	12 or 24	48	48	24	
10-year risk of cirrhosis (%)	28.0	4.9	16.1	10.8	6.8	17.9	10.9	23.1	12.9	10.9	45.1
10-year risk of HCC (%)	15.0	2.9	9.2	6.6	3.9	10.2	6.2	13.2	7.4	6.2	26.6
Life expectancies (years)	15.90	18.20	17.02	17.57	18.01	16.93	17.61	16.38	17.35	17.61	13.93
QALYs	11.36	14.54	12.92	13.68	14.32	12.80	13.76	12.02	13.35	13.74	8.88
Lifetime cost (€)	54 064	29 933	46 313	38 606	25 964	39 990	31 154	50 854	44 599	34 005	50 834

The new protocol for treatment was classified considering the viral genotypes, viral load, and RVR. The genotype 1-infected patients with a low viral load (the weighted average of subgroups B and C) and patients infected with the genotypes 2 or 3 (the weighted average of subgroup D and E) in the new protocol presented the most prolonged QALYs and a more reduced lifetime cost compared with the corresponding groups in the standard protocol. The costs and benefits were discounted at 3%/year.
HCC, hepatocellular carcinoma; QALYs, quality-adjusted life years; RVR, rapid virologic response; SVR, sustained virologic response.
[a]The weighted average using the rate of RVR.
[b]Viral load not considered.

Table 5 The probable ranges of the cost-effectiveness measures, which were determined by the results of the sensitivity analysis

	Genotype 1	Genotype 2 or 3
Difference of QALYs (new protocol–standard protocol)		
Base-case analysis	0.33	0.02
Sensitivity analysis		
Lower limit of SVR in the new protocol for treatment	−0.42	−0.41
Lower limit of RVR in the new protocol for treatment	0.08	−0.07
Other sensitivity analysis	0.22 to 1.07	0.02 to 0.44
Difference of lifetime cost (€) (new protocol–standard protocol)		
Base-case analysis	−5993	−2851
Sensitivity analysis	−9765 to −2169	−5517 to −109

The base-case results in the new protocol for treatment presented superiority both in lifetime cost and QALYs in comparison to those in the standard protocol. A one-way sensitivity analysis showed that QALYs in the new protocol for treatment could be shortened compared with the standard protocol when the rate of SVR or RVR in the former achieved the lower limit of the 95% confidence interval. The lifetime costs were reduced at any of the results of the sensitivity analysis.
Lower limit, lower limit of the 95% confidence interval; QALYs, quality-adjusted life years; RVR, rapid virologic response; SVR, sustained virologic response.

peginterferon plus ribavirin were reported to be lower in these shorter courses than in the standard protocols. Mangia *et al.* [14] suggested that a 12-week course of peginterferon α-2b plus ribavirin therapy was effective for patients infected with genotype 2 or 3 with RVR. Zeuzem *et al.* [13] showed that a 24-week course of peginterferon α-2b plus ribavirin therapy for patients infected with genotype 1 with a low viral load and RVR achieved a similar SVR rate of 89% to those in the historical control group (treatment for 48 weeks). After the publication of the report by Zeuzem *et al.* [13], the European Commission approved revised dosing instructions which prescribed a shorter (24-week) course of peginterferon α-2b plus ribavirin therapy for patients with genotype 1 and low viral load, who achieved RVR [37]. From these studies, it was clear that short courses of combination therapy are as effective as standard courses when patients have achieved an RVR. More successful cases of treatment with this regimen, however, still need to be accumulated, to confirm its effectiveness. The number of reports demonstrating the effectiveness of shorter courses of treatment in achieving an RVR are still too few to justify confirmations. In addition, it is important that clinical effectiveness should be complemented by economic evaluations, such as lifetime costs and QALYs. Wong *et al.* [38] reported that 24-week treatment for genotype 1-infected patients who had a low pretreatment level of viral load and had achieved RVR can reduce the cost in the combination therapy by at least 27%. Furthermore, we analyzed the lifetime costs and QALYs for 30 years, systematically evaluating RVRs for both genotype 1 with a low viral load and genotypes 2 and 3. The lifetime costs mostly depend on the treatment costs of the combination therapy in our study. When the cost of the combination therapy was reduced by 50% in our model, the lifetime cost could be reduced by €3190 (a saving of 9.1%) in genotype 1 with a low viral load and by €1493 (a saving of 5.0%) in genotypes 2 and 3

compared with costs for similar treatment groups in the standard protocol. Combination therapy, however, requires a dose reduction to some extent, and our assumption of −50% in cost was considered to be a minimum.

We defined the treatment duration for patients with genotypes 2 and 3 with an RVR of 12 weeks, but it remains controversial. Dalgard *et al.* [39] assessed 14 weeks of combination therapy for patients infected with genotypes 2 or 3 with RVR, and showed that these patients achieved the SVR rate of 90% after a 14-week course of treatment. On the other hand, Wagner *et al.* [40] reported the efficacy of 16 weeks of treatment with peginterferon α-2a plus ribavirin in patients who were infected with genotype 2 or 3 and who had achieved an RVR compared with the standard 24 weeks of treatment. When we assumed the treatment duration for patients infected with genotypes 2 or 3 in the new protocol to be 16 weeks, the lifetime cost was estimated as €32 081. This is still lower than the standard protocol lifetime cost for treatment of €34 005. The new protocol for treatment with a 16-week duration would also, therefore, be cost-effective.

Finally, the treatment costs for patients who relapsed after treatment or had detectable HCV at week 24 were considered to be wasted costs, which had already been incurred. They were not factored into current investment decisions. Davis *et al.* [41] reported that no patient achieved an SVR, even if the HCV-RNA became negative at week 24, if it was still detectable at week 12, or if it had decreased to less than $2 \log_{10}$ of the pretreatment levels. We can, thus, save more lifetime cost if we incorporate these data in our model. Not all of these costs, however, are thought to be wasted. Recent therapeutic reports for combination therapy with peginterferon α-2a and ribavirin have suggested that an extended 72 weeks of treatment (48 plus 24 weeks) for genotype 1-infected patients, who did not become HCV-RNA negative at week 12 but became negative at week 24, statistically improved the SVR rate and also decreased the relapse rate, compared with the standard 48 weeks of treatment [42]. In that study, the reported SVR rate of 29% in the extended 72-week treatment was significantly higher than the 17% rate in the standard 48-week treatment. Conversely, the relapse rate was reported to be 40% in the extended 72-week treatment, which was significantly lower than the 64% rate in the standard 48-week treatment. These data were obtained from treatment with peginterferon α-2a plus ribavirin and cannot be incorporated directly into our model: nevertheless the cost-effectiveness is thought to be worth an investigation, as the effectiveness can be improved and wasted cost reduced despite the additional costs. Further studies will be needed to clarify the impacts of such unrecoverable costs.

References

1 World Health Organization (WHO). Available at: *http://www.who.int/vaccine_research/disease/viral_cancers/en/index2/htm*. Accessed 13 January 2007.
2 National Institutes of Health. Consensus Development Conference Statement: Management of Hepatitis C, June 2002. Available at: *http://www.consensus.nih.gov* Accessed 2 March 2007.
3 El-Serag HB, Devila JA, Petersen NJ, McGlynn KA. The continuing increase in the incidence of hepatocellular carcinoma in the United States: an update. *Ann Intern Med* 2003; 139:817–824.
4 Vecchia C, Lucchini F, Franceschi S, Negri E, Levi F. Trends in mortality from primary liver cancer in Europe. *Eur J Cancer* 2000; 36:909–915.
5 Manns MP, McHutchison JG, Gordon SC, Rustgi VK, Shiffman M, Reindollar R, *et al.* Peginterferon alfa-2b plus ribavirin compared with interferon alfa-2b plus ribavirin for initial treatment of chronic hepatitis C: a randomized trial. *Lancet* 2001; 358:958–965.
6 Pockros PJ, Carithers R, Desmond P, Dhumeaux D, Fried MW, Marcellin P, *et al.* Efficacy and safety of two-dose regimens of peginterferon alpha-2a compared with interferon alpha-2a in chronic hepatitis C: a multicenter, randomized controlled trial. *Am J Gastroenterol* 2004; 99:1298–1305.
7 Strader DB, Wright T, Thomas DL, Seeff LB. The American Association for the Study of Liver Diseases. Diagnosis, management, and treatment of hepatitis C. *Hepatology* 2004; 39:1147–1171.
8 Sullivan SD, Craxi A, Alberti A, Guiliani G, Decarli C, Wintfeld N, *et al.* Cost effectiveness of peginterferon alpha-2a plus ribavirin versus interferon alpha-2b plus ribavirin as initial therapy for treatment-naive chronic hepatitis C. *Pharmacoeconomics* 2004; 22:257–265.
9 Buti M, Medina M, Casado MA, Wong JB, Fosbrook L, Esteban R. A cost-effectiveness analysis of peginterferon alfa-2b plus ribavirin for the treatment of naive patients with chronic hepatitis C. *Aliment Pharmacol Ther* 2003; 17:687–694.
10 Siebert U, Sroczynski G, Rossol S, Wasem J, Ravens-Sieberer U, Kurth BM, *et al.* Cost effectiveness of peginterferon alpha-2b plus ribavirin versus interferon alpha-2b plus ribavirin for initial treatment of chronic hepatitis C. *Gut* 2003; 52:425–432.
11 Wong JB, Davis GL, McHutchison JG, Manns MP, Albrecht JK. Economic and clinical effects of evaluating rapid viral response to peginterferon alfa-2b plus ribavirin for the initial treatment of chronic hepatitis C. *Am J Gastroenterol* 2003; 98:2354–2362.
12 Buti M, Casado MA, Fosbrook L, Esteban R. Financial impact of two different ways of evaluating early virological response to peginterferon-alpha-2b plus ribavirin therapy in treatment-naive patients with chronic hepatitis C virus genotype 1. *Pharmacoeconomics* 2005; 23:1043–1055.
13 Zeuzem S, Buti M, Ferenci P, Sperl J, Horsmans Y, Cianciara J. Efficacy of 24 weeks treatment with peginterferon alfa-2b plus ribavirin in patients with chronic hepatitis C infected with genotype 1 and low pretreatment viremia. *J Hepatol* 2006; 44:97–103.
14 Mangia A, Santoro R, Minerva N, Ricci GL, Carretta V, Persico M, Vinelli F. Peginterferon alfa-2b and ribavirin for 12 vs. 24 weeks in HCV genotype 2 or 3. *N Eng J Med* 2005; 352:2609–2617.
15 Nainan OV, Alter MJ, Kruszon-Moran D, Gao FX, Xia G, Mcquillan G, *et al.* Hepatitis C virus genotypes and viral concentrations in participants of a general population survey in the United States. *Gastroenterology* 2006; 131:478–484.
16 Beck JR, Pauker SG. The medical process in medical prognosis. *Med Decis Making* 1983; 3:419–458.
17 Sonnenberg FA, Beck JR. Markov models in medical decision making: a practical guide. *Med Decis Making* 1993; 13:322–338.
18 Takahashi M, Yamada G, Miyamoto R, Doi T, Endo H, Tsuji T. Natural course of chronic hepatitis C. *Am J Gastroenterol* 1993; 88:240–243.
19 Yousuf M, Nakano Y, Tanaka E, Sodeyama T, Kiyosawa K. Persistence of viremia in patients with type-C chronic hepatitis during long-term follow-up. *Scand J Gastroenterol* 1993; 27:812–816.
20 Kobayashi M, Tanaka E, Sodeyama T, Urushihara A, Matsumoto A, Kiyosawa K. The natural course of chronic hepatitis C: a comparison between patients with genotype 1 and 2 hepatitis C virus. *Hepatology* 1996; 23:695–699.
21 Shibata M, Morizane T, Uchida T, Yamagami T, Onozuka Y, Nakano M, *et al.* Irregular regeneration of hepatocytes and risk of hepatocellular carcinoma in chronic hepatitis and cirrhosis with hepatitis-C-virus infection. *Lancet* 1998; 351:1773–1777.
22 Kaneko S, Unoura M, Takeuchi M, Terasaki S, Ogino H, Matsushita E, Kobayashi K. The role of hepatitis C virus in hepatocellular carcinoma in Japan. *Intervirology* 1994; 37:108–113.
23 Fattovich G, Giustina G, Degos F, Tremolada F, Diodati G, Almasio P. Morbidity and mortality in compensated cirrhosis type C: a retrospective follow-up study of 384 patients. *Gastroenterology* 1997; 112:463–472.

24 Serfaty L, Aumaitre H, Chazouilleres O, Bonnand AM, Rosmorduc O, Poupon RE, *et al.* Determinants of outcome of compensated hepatitis C virus-related cirrhosis. *Hepatology* 1998; 27:1435–1440.

25 Kato Y, Nakata K, Omagari K, Furukawa R, Kusumoto Y, Mori I, *et al.* Risk of hepatocellular carcinoma in patients with cirrhosis in Japan. Analysis of infectious hepatitis viruses. *Cancer* 1994; 74:2234–2238.

26 Nishiguchi S, Kuroki T, Nakatani S, Morimoto H, Takeda T, Nakajima S, *et al.* Randomised trial of effects of interferon-α on incidence of hepatocellular carcinoma in chronic active hepatitis C with cirrhosis. *Lancet* 1995; 346:1051–1055.

27 Ikeda K, Saitoh S, Koida I, Arase Y, Tsumota A, Chayama K, *et al.* A multivariate analysis of risk factors for hepatocellular carcinogenesis: a prospective observation of 795 patients with viral and alcoholic cirrhosis. *Hepatology* 1993; 18:47–53.

28 Tanaka K, Sakai H, Hashizume M, Hirohata T. A long-term follow-up study on risk factors for hepatocellular carcinoma among Japanese patients with liver cirrhosis. *Jpn J Cancer Res* 1998; 89:1241–1250.

29 Miyakawa H, Izumi N, Marumo F, Sato C. Roles of alcohol, hepatitis virus infection, and gender in the development of hepatocellular carcinoma in patients with liver cirrhosis. *Alcohol Clin Exp Res* 1996; 20:91A–94A.

30 Grieve R, Roberts J, Wright M, Sweeting M, DeAngelis D, Rosenberg W, *et al.* Cost effectiveness of interferon alpha or peginterferon alpha with ribavirin for histologically mild chronic hepatitis C. *Gut* 2006; 55: 1332–1338.

31 OECD. *Main economic indicators.* Paris, France: OECD; 2006.

32 Sangiovanni A, Prati GM, Fasani P, Ronchi G, Romeo R, Manini M. The natural history of compensated cirrhosis due to hepatitis C virus: a 17-year cohort study of 214 patients. *Hepatology* 2006; 43:1303–1310.

33 Benvegnu L, Gios M, Boccato S, Alberti A. Natural history of compensated viral cirrhosis: a prospective study on the incidence and hierarchy of major complications. *Gut* 2004; 53:744–749.

34 Abridged life table for Japan. 2004. Tokyo: Statistics and Information Department, Minister's Secretariat, Ministry of Health, Labour, and Welfare, 2005.

35 Weinstein MC, Siegel JE, Gold MR, Kamlet MS, Russell LB. Recommendations of the Panel on Cost-effectiveness in Health and Medicine. *JAMA* 1996; 276:1253–1258.

36 Yano M, Kumada H, Kage M, Ikeda K, Shimamatsu K, Inoue O, *et al.* The long-term pathological evolution of chronic hepatitis C. *Hepatology* 1996; 23:1334–1340.

37 Short course pegintron plus rebetol approved in Europe for HCV patients with genotype 1 and low viral load. Available at: *http://www.hivandhepatitis.com/hep_c/news/2005/ad/100705_a.html.* Accessed 13 January 2007.

38 Wong JB, Zeuzem S, Manns MP, Albrecht JK. Clinical and economic implications of a 4-week viral negative response to peginterferon alfa-2b plus ribavirin for chronic hepatitis C and genotype 1 with low viral load. *Hepatology* 2005; 42:679A.

39 Dalgard O, Bjøro K, Hellum KB, Myrvang B, Ritland S, Skaug K, *et al.* Treatment with pegylated interferon and ribavirin in HCV infection with genotype 2 or 3 for 14 weeks: a pilot study. *Hepatology* 2004; 40: 1260–1265.

40 Wagner MV, Huber M, Berg T, Hinrichsen H, Rasenack J, Heintges T, *et al.* Peginterferon-α-2a (40KD) and ribavirin for 16 or 24 weeks in patients with genotype 2 or 3 chronic hepatitis C. *Gastroenterology* 2005; 129:522–527.

41 Davis GL, Wong JB, McHutchson JG, Manns MP, Harvey J, Albrecht J. Early virologic response to treatment with peginterferon alfa-2b plus ribavirin in patients with chronic hepatitis C. *Hepatology* 2003; 38:645–652.

42 Berg T, Wagner MV, Nasser S, Sarrazin C, Heintges T, Gerlach T, *et al.* Extended treatment duration for hepatitis C virus type 1: comparing 48 versus 72 weeks of peginterferon-alfa-2a plus ribavirin. *Gastroenterology* 2006; 130:1086–1097.

ELSEVIER

Journal of Hepatology 48 (2008) 255–265

Journal of Hepatology

www.elsevier.com/locate/jhep

Temporal treatment with interferon-β prevents hepatocellular carcinoma in hepatitis B virus X gene transgenic mice☆

Kazuhide Yamazaki[1,†], Kenta Suzuki[1,‡], Shogo Ohkoshi[1,*], Masahiko Yano[1], So Kurita[1], Yo-hei Aoki[1], Ken Toba[2], Masa-aki Takamura[1], Satoshi Yamagiwa[1], Yasunobu Matsuda[1], Yutaka Aoyagi[1]

[1] *Division of Gastroenterology and Hepatology, Graduate School of Medical and Dental Sciences of Niigata University, 1-754, Asahimachi-Dori, Niigata-city 951-8122, Japan*

[2] *Division of Hematology, Graduate School of Medical and Dental Sciences of Niigata University, 1-754, Asahimachi-Dori, Niigata-city 951-8122, Japan*

***Background/Aims*: The preventive effect of interferon (IFN) against hepatocellular carcinoma (HCC) has been confirmed clinically. We sought to determine whether the temporal administration of IFN-β prevents hepatocarcinogenesis in a mouse model where HCC develops without necroinflammation.**

***Methods*: Hepatocarcinogenic mice that are transgenic for the hepatitis B virus X gene (HBx-Tg) were treated with IFN-β or saline (control) for three months, from 3 to 6 months of age, and the incidence of HCC was determined at 18 months of age. The effects of IFN-β on DNA synthesis and apoptosis were tested.**

***Results*: The incidence of HCC was significantly lower in the IFN-β-treated mice than the controls (0 vs. 50%, $P < 0.01$). Inhibition of DNA synthesis in hepatocytes by IFN-β was observed in the livers of HBx-Tg, without any significant induction of apoptosis. Although the treatment of IFN-β was temporal, the number of hepatocytes with DNA synthesis remained lower 3 and 12 months later in life.**

***Conclusions*: Temporal administration of IFN-β has a significant preventive effect on the occurrence of HCC in a mouse model where HCC develops without inflammation. The mechanisms are the inhibition of DNA synthesis and cell cycle progression of hepatocytes.**

***Keywords*: Interferon-β; Hepatocarcinogenesis; Temporal treatment; Hepatitis B virus X gene; Transgenic mouse; DNA synthesis; Cell cycle; Primary hepatocyte culture; WRL-68**

1. Introduction

Hepatocellular carcinoma (HCC) is one of the most common malignancies worldwide [1]. Necroinflammation caused by hepatitis viruses or other toxic agents induces a broad variety of genetic alterations which ultimately lead to the clinical manifestation of HCC [2–4].

A number of studies have shown that interferon (IFN) treatment may prevent hepatocarcinogenesis in patients with chronic hepatitis C [5–8] and hepatitis B [9]. Inhibition of HCC development has been shown clearly in patients with chronic hepatitis C who achieved

Received 8 May 2007; received in revised form 20 September 2007; accepted 21 September 2007; available online 20 November 2007
Associate Editor: K. Koike

☆ The authors who have taken part in the research of this paper declared that they do not have a relationship with the manufacturers of the drug involved either in the past or present and they did not receive funding from the manufacturers to carry out their research. They did not receive funding from any source to carry out this study.

* Corresponding author. Tel.: +81 25 227 2204; fax: +81 25 227 0776.
E-mail address: okoshi@med.niigata-u.ac.jp (S. Ohkoshi).
† Takeda General Hospital, Aizu-Wakamatsu city, 965-8585, Japan.
‡ Kuwana Hospital, Niigata-city, 950-0032, Japan.

0168-8278/$32.00
doi:10.1016/j.jhep.2007.09.012

viral eradication or normalization of alanine aminotransferase (ALT) [5–8] as well as those who could not achieve these outcomes [10].

The mechanisms of the inhibitory effects of IFN on HCC involve multiple factors, which include: (i) suppression of viral replication, (ii) immunomodulative effects, and (iii) direct antiproliferative activity such as the induction of apoptosis or inhibition of the cell cycle [11,12]. Although the antiproliferative activities of IFN in the context of anti-tumor effects have been investigated extensively using HCC-derived cell lines [13–16], only a few studies have examined this effect on primary hepatocytes [17]. Unfortunately, there have been no studies extrapolating this approach to the preventive action of IFN on HCC.

IFN-β belongs to the type-I IFNs [11,12] and has been reported to inhibit the recurrence of HCC in patients with chronic hepatitis [18]. Although the biological functions of IFN-β are similar to those of IFN-α, more pronounced growth-inhibitory effects have been reported [19–23].

The question we asked was whether the antiproliferative effect of IFN-β has a preventive role in the development of HCC, even with temporal administration. To investigate this hypothesis, we used a hepatocarcinogenic transgenic mouse model which contained the hepatitis B virus X (HBx) gene (HBx-Tg) [24–26] and in which there was no necroinflammatory activity in the pathology of liver. Enhanced DNA synthesis and apoptosis may eventually result in the development of HCC from 12 months of age [25].

So far, a few reports have addressed the preventive effect of IFN *in vivo* [27–29] but none has successfully shown the inhibition of hepatocarcinogenesis by temporal treatment with IFN. Merle et al. showed a preventive effect of IFN-α for HCC by continuous treatment of a highly-hepatocarcinogenic transgenic mouse [27,28]. However, because they gave the mice lifelong IFN treatment, both a tumor-killing effect and an antiproliferative effect on normal pre-cancerous hepatocytes might have contributed to the anti-hepatocarcinogenic effect.

The aim of this study was to clarify whether short term-treatment with IFN-β carried out in our mouse model at a young age when the livers of the animals were free from cancers and precancerous lesion, had a preventive effect against HCC.

2. Materials and methods

2.1. In vivo experimental protocol

Human and mouse IFN-β were kindly supplied by Toray Co., Ltd (Tokyo, Japan). A highly-hepatocarcinogenic mouse model (HBx-Tg) was used [24]. The experimental protocol is shown in Fig. 1A: 5000 U/gram body weight of mouse-IFN-β (23 mice, Male:Female = 12:11) or saline (17 mice, M:F 6:11) was administered intraperitoneally [30] to three-month-old HBx mice three times per week for three months. Four (M:F = 2:2) and three (M:F = 1:2) mice from the respective groups were sacrificed at the end of treatment (6 months old). Four (M:F = 2:2) mice from each group were sacrificed 3 months after the end of the treatment (9 months old), otherwise mice (M:F = 8:7 for IFN-β and M:F = 3:7 for controls) were sacrificed at 18 months of age.

All the experimental protocols were approved by the Institutional Animal Care and Use Committee of Niigata University and performed in accordance with the National Institutes of Health Guidelines.

2.2. Hepatocyte proliferation assay in vivo and in vitro

HBx-Tg were treated at 12 weeks of age with 5000 U/gram body weight IFN-β or saline intraperitoneally for 10 days, and water with 1 mg/ml bromodeoxyuridine (BrdU) was given to the mice for the last 5 days prior to sacrifice [31]. Paraffin-embedded liver sections were subjected to staining with anti-BrdU (Dako, Japan). Cell proliferation also was assessed in the livers of the mice sacrificed at 18 months of age by the incubation of the slides with anti-PCNA antibodies (Dako) at 4 °C overnight.

Primary cultured hepatocytes were prepared from 6-week-old mouse livers using a conventional collagenase perfusion method [32].

BrdU incorporation assays in primary hepatocyte culture were carried out as described previously [33,34].

2.3. Quantification of apoptosis

Quantitative analysis of apoptosis was performed by a terminal deoxynucleotidyl transferase-mediated nick end-labeling (TUNEL) method (In Situ apoptosis Detection kit, Chemicon International, Temecula, CA) for mouse hepatocytes *in vivo* and *in vitro*, and by caspase-Glo™ 3/7 assay (Promega, Madison, WI) for WRL-68 cells. Liver tissues from the HBx-Tg, obtained using the protocol for the cell proliferation analysis, also were subjected to TUNEL analysis. WRL-68 cells were incubated with or without IFN-β for 3 or 6 h and assayed by a luminometer (Luminescencer-JNR, AB 2100, Atto, Japan).

2.4. Effect of IFN-β on cell proliferation and cell cycle in a normal hepatocyte cell line

A normal human hepatocyte cell line (WRL-68: American Type Culture Collection, Manassas, VA) [35] was obtained commercially.

To analyze the effect of IFN-β on WRL-68 cell proliferation, the number of viable cells was determined by a modified MTT assay (Cell counting kit-8, Dojindo, Japan) according to the manufacturer's instructions.

For cell cycle analysis, a time chase experiment was carried out on cells that had incorporated BrdU to determine the effect of IFN-β on the cell cycle [36–38].

2.5. Quantification of HBx mRNA using TaqMan-PCR

Primary hepatocytes (1×10^5 cells/ml) obtained from an HBx-Tg were cultured with or without 100,000 U/ml IFN-β. Cells were harvested at 0, 1, and 3 h, and RNA was extracted. Similarly, RNA was extracted from IFN-β or PBS treated-mice (described in Section 2.2). After digestion with DNase, one microgram of RNA was converted to cDNA (Transcriptor first strand cDNA synthesis kit, Roche, Germany). Aliquots of cDNA samples were subjected to *Taq*Man-PCR using a light cycler (Roche). Primers for detecting HBx mRNA were 5′-CCCGTCTGTGCCTTCTCA-3′ (sense) and 5′-AGCAATGTCAA CGACCGACC-3′ (antisense), and the (*Taq*Man) probe: 6FAMS 5′-C CGTGTGCACTTCGCT-3′ TAMRA to detect amplicons of 148 bps. Mouse β-actin mRNA was quantified as an endogenous control. PCR protocols were as follows: denaturation at 95 °C for 30 s followed by 40 cycles of 95 °C for 5 s and 60 °C for 15 s. HBx mRNA levels in each sample were standardized by levels of β-actin mRNA at each time point. For the RNA obtained from primary hepatocytes, values from six samples were obtained at each time point (two experiments in triplicate), and the relative values of HBx mRNA at 1 and 3 h to the baseline levels (means ± SD) were calculated. Statistical comparisons were made between the baseline level of HBx mRNA and >that obtained at each time point. For the RNA obtained from the HBx-Tg liver, six (IFN-treated) and five (saline) samples were analyzed.

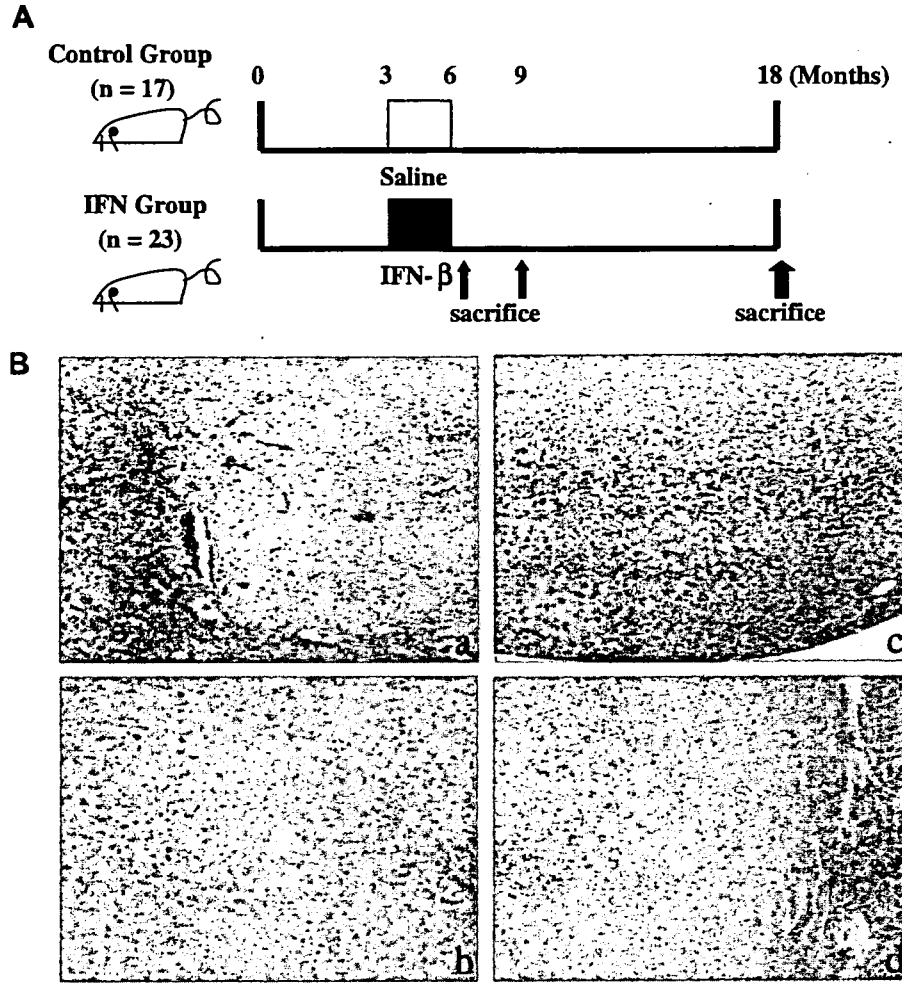

Fig. 1. (A) The experimental protocol. 5000 U/gram body weight of mouse-IFN-β or saline was administered intraperitoneally to 3-month-old HBx mice three times per week for 3-months. (B) Representative histological sections of two adenomas (a,c) and HCCs (b,d) observed in these mice. Paraffin sections (7 μM) were stained with hematoxylin–eosin and examined for the presence and the severity of pathological lesions under a light microscope. HCCs were diagnosed when recognized as expanding nodules in the liver and confirmed histologically. Adenomas were defined macroscopically as nodules of a few millimeters and confirmed microscopically as tumors with low-grade atypia. (C) Representative liver histology obtained from a control HBx and IFN-β-treated HBx-Tg at 3 (before treatment, a), 6 (at the end of treatment, b and d), and 18 months (c and e) of age. Note that histological abnormalities such as ballooning of hepatocytes (upper arrow), piknotic nucleus (lower arrow), and pleomorphy were less conspicuous in the IFN-β-treated mice (d and e) than the untreated HBx-Tg (b and c) at both 6 and 18 months of age. To assess these histological changes quantitatively, we estimated the degree of these pathological changes subjectively and scored as "index of atypism" from grade 0 to 10 in each animal sacrificed immediately after the IFN-treatment and at 18 month of age. Although not significant, the indices were lower in the IFN-β treated mice than in the control mice both immediately after treatment (0.9 ± 1.2 vs. 1.4 ± 1.6) and at 18 months of age (1.7 ± 2.5 vs. 3.6 ± 3.6). (D) (a) Cell proliferation was assessed with anti-PCNA antibodies for each mouse liver obtained at 3 (before IFN-treatment, $n = 5$), 6 (immediately after treatment), 9 (3 months after treatment) and 18 months (12 months after treatment). PCNA-positive hepatocytes were counted in the normal (non-tumorous) part of the liver in 20 randomly selected light-microscope fields at 400× magnification and the average number per mouse was obtained. The labeling index was the highest in the HCC tissues (data not shown). Data shown are means ± SD. It was significantly lower in the IFN-β-treated mice than in the control mice at every point after the treatment with IFN-β ($^*P < 0.05$). (b) The number of apoptotic hepatocytes was assessed in these mice using the TUNEL-method. Apoptotic cells were counted and analyzed in the same manner with PCNA-staining.

2.6. Western blot analysis

Proteins were isolated from mouse primary hepatocytes and the aliquots were separated by SDS–PAGE. The samples were electroblotted onto polyvinylidene fluoride (PVDF) membranes (Immobilon-P, Millipore, Bedford, MA). After incubation with primary antibodies [anti-Stat1, anti-phosphorylated Stat1, anti-Stat3, anti-phosphorylated Stat3, anti-PCNA, (Santa Cruz; Santa Cruz, CA), anti-β-actin (Sigma), anti-p44/42 MAPK, anti-phospho-p44/42MAPK (Cell Signaling Technology, Beverly, MA)], membranes were incubated with appropriate secondary antibodies. Proteins were visualized using ECL chemiluminescence (GE Healthcare).

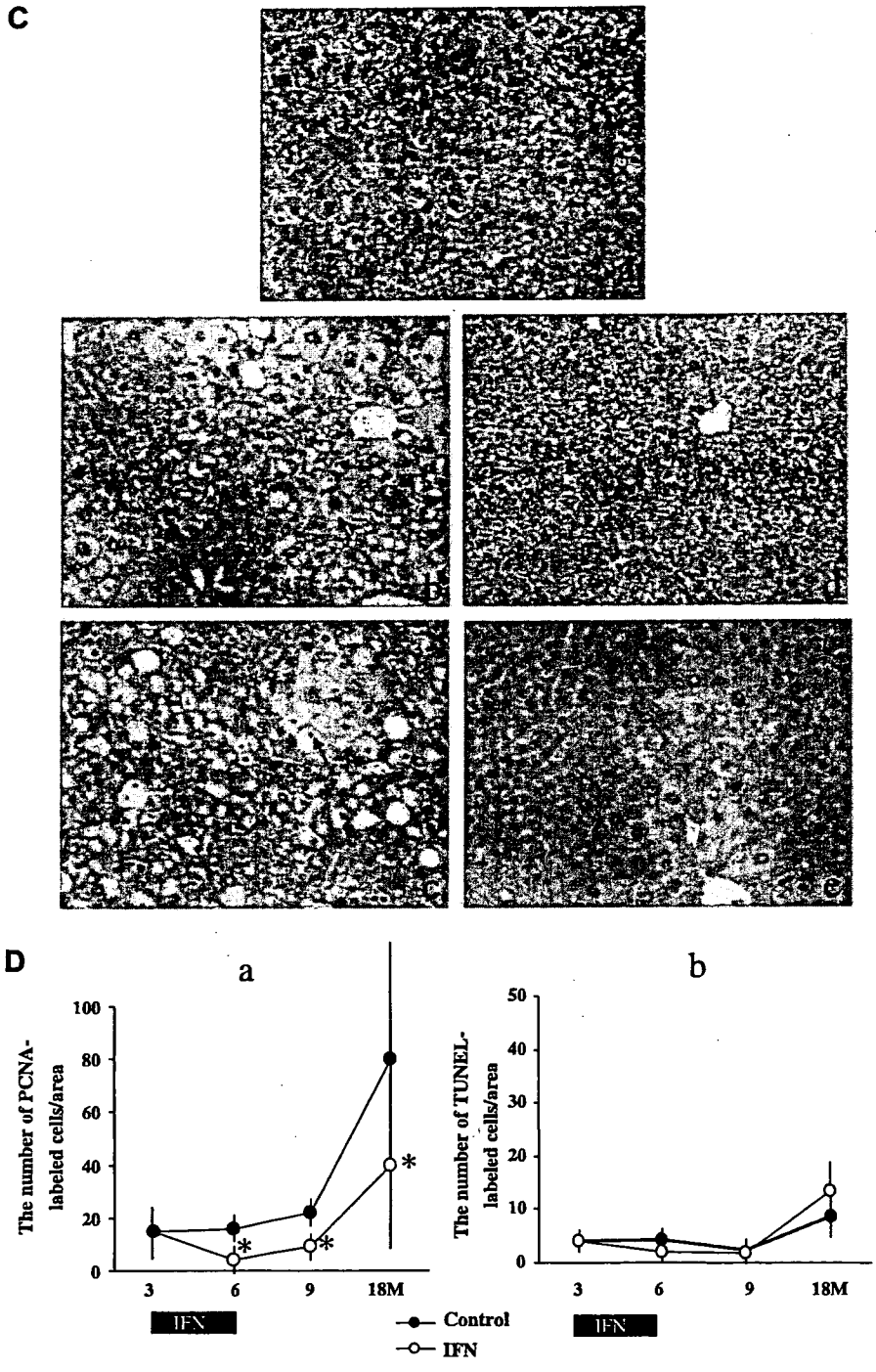

Fig. 1 (*continued*)

2.7. Statistical analysis

The results were expressed as means ± standard deviation (SD) obtained from multiple independent experiments. Yates χ^2 test, exact Fischer tests, Student's *t*-test, or Mann–Whitney's non-parametric test were used for statistical analysis as appropriate. Advance of $P < 0.05$ was considered statistically significant.

3. Results

3.1. Early treatment with IFN-β decreases the incidence of HCC in HBx-Tg

Our preliminary results from microscopy show that HCC does not arise in the HBx mice until they reach

12 months of age and precancerous adenomas do not arise until 6 months of age (unpublished observations). The incidence of HCC and adenomas in the mice at 18 months of age, after treatment with IFN-β or saline, is shown in Table 1. Although the number of female mice, that are less prone to HCC in this model [24], was higher in the control group, the incidence of HCC was significantly lower in the IFN-β treated group (50% for the control, and 0% for IFN-β-treated) ($P < 0.01$). Representative histological sections of two adenomas and two HCCs are shown in Fig. 1B. Pathological abnormalities of liver tissue, such as the presence of atypical hepatocytes that show pleomorphy and ballooning (arrow), were more conspicuous in the control mice than in the IFN-β treated mice at the end of treatment (6 months) (Fig. 1C). These changes, as well as the appearance of piknotic nuclei (arrow), were more evident in the control mouse livers at the time of sacrifice (18 months), whereas slower progress of abnormalities was observed in the IFN-β-treated mice. Cell proliferation was assessed by immunostaining of PCNA in liver tissues. The number of labeled hepatocytes was significantly lower immediately after treatment with IFN-β (Fig. 1D-a) and, even though the IFN treatment was temporal, the number of labeled hepatocytes remained significantly lower in the IFN-treated mice at 3 and 12 months after treatment ($P < 0.05$). In addition, the numbers of labeled cells in the normal liver tissues tended to be higher in those with HCC than without HCC (180 ± 138 vs. 56 ± 44) ($P = 0.14$). Thus, the increase of PCNA-labeled cells might reflect the cancer-prone tendency of the liver.

We also assessed the number of apoptotic hepatocytes in these mice using TUNEL assay (Fig. 1D-b). In contrast to the PCNA staining, there was no significant difference in the number of TUNEL-positive hepatocytes between IFN-treated and control mice at each point.

3.2. Inhibition of DNA synthesis by IFN-β in hepatocyte in vivo and in vitro

We investigated the effect of IFN-β on DNA synthesis and the apoptosis of hepatocytes *in vivo* (Fig. 2). HBx-Tg had a significantly higher number of hepatocytes that had incorporated BrdU than non-transgenic control mice of the same age (839 ± 194 vs. 148 ± 95 in the whole slides per mouse, $P < 0.05$). Administration of IFN-β to 12-week-old HBx mice for 10 days suppressed the numbers of BrdU-positive hepatocytes compared to non-treated control HBx-Tg ($P < 0.01$) (Fig. 2A and B). However, the numbers of TUNEL-positive (apoptotic) hepatocytes were not significantly affected (Fig. 2C).

In order to isolate the effect of IFN-β observed in vivo, where the biological effects of IFN might be complex, we examined the effect of IFN-β on primary mouse hepatocytes derived from HBx-Tg (Fig. 3). The number of BrdU positive cells decreased in the presence of 1000 U IFN-β ($P < 0.05$) (Fig. 3A and B) and was more significant with 10,000 U IFN-β ($P < 0.01$, data not shown). A decrease in PCNA following IFN-β treatment, measured by Western blot analysis (an approximately twofold change by densitometry using the relative ratio to β-actin), was consistent with the inhibition of DNA synthesis (Fig. 3C). The number of apoptotic cells increased by the treatment with IFN-β, but not significantly (Fig. 3B).

Table 1
Liver tumor incidence in IFN-β treated and control mice

		Adenomas	HCC
Control	($n = 10$, M:F = 3:7)	2 (20%)	5 (50%)[a]
IFN	($n = 15$, M:F = 8:7)	2 (13%)	0 (0%)[a]

Note: All the IFN-treated mice were injected with IFN-β i.p.(5000 U/gram body weight) 3 times/week for 3 months from 3 months of age. HCC; hepatocellular carcinoma. The greatest diameters of the HCCs were 11,11,15,16, and 23 mm, whilst those of the adenomas were all less than 3 mm. One of the control mice had both HCC and adenoma. HCCs were found in 2 males and 3 females. The adenomas found in control and IFN-treated mice were in 1 male and 1 female.

[a] $P < 0.01$, Exact Fischer test.

3.3. Growth-inhibitory effect of IFN-β on the human normal hepatocyte cell line was attributable to cell cycle arrest at S phase

In order to analyze the antiproliferative effect of IFN-β in human hepatocytes quantitatively according to changes in rate of cell-growth and dynamically by flow cytometry analysis in human hepatocytes, we chose to use the immortalized normal human hepatocyte cell line WRL-68 [35,39]. In modified MTT assays, at least 10,000 U/ml of IFN-β showed a significant inhibitory effect on the growth of WRL-68 cells after 48 h incubation (Fig. 4A). We tested the apoptotic effect of IFN-β on these cells by detecting caspase 3/7 activity, but could not see any increase in caspase activity after treatment with IFN-β (Fig. 4B). We analyzed the cell cycle distribution by flow cytometry following IFN-β treatment (Fig. 4C). A time chase experiment was carried out on cells that had incorporated BrdU to measure the effect of IFN-β on the cell cycle. WRL-68 cells in the S phase (2 N) shifted gradually to G2/M phase (4 N) and most of the cells were in this phase at 6 h, although a small population reappeared at G1 (upper panel, dotted circle). However, most of the IFN-β-treated cells remained in the S phase even at 6 h (lower panel). This was considered an S phase block of WRL-68 cells by IFN-β.

3.4. The level of HBx gene mRNA was not affected by IFN-β

We sought changes in the levels of HBx mRNA in primary hepatocyte culture and livers from HBx-Tg by

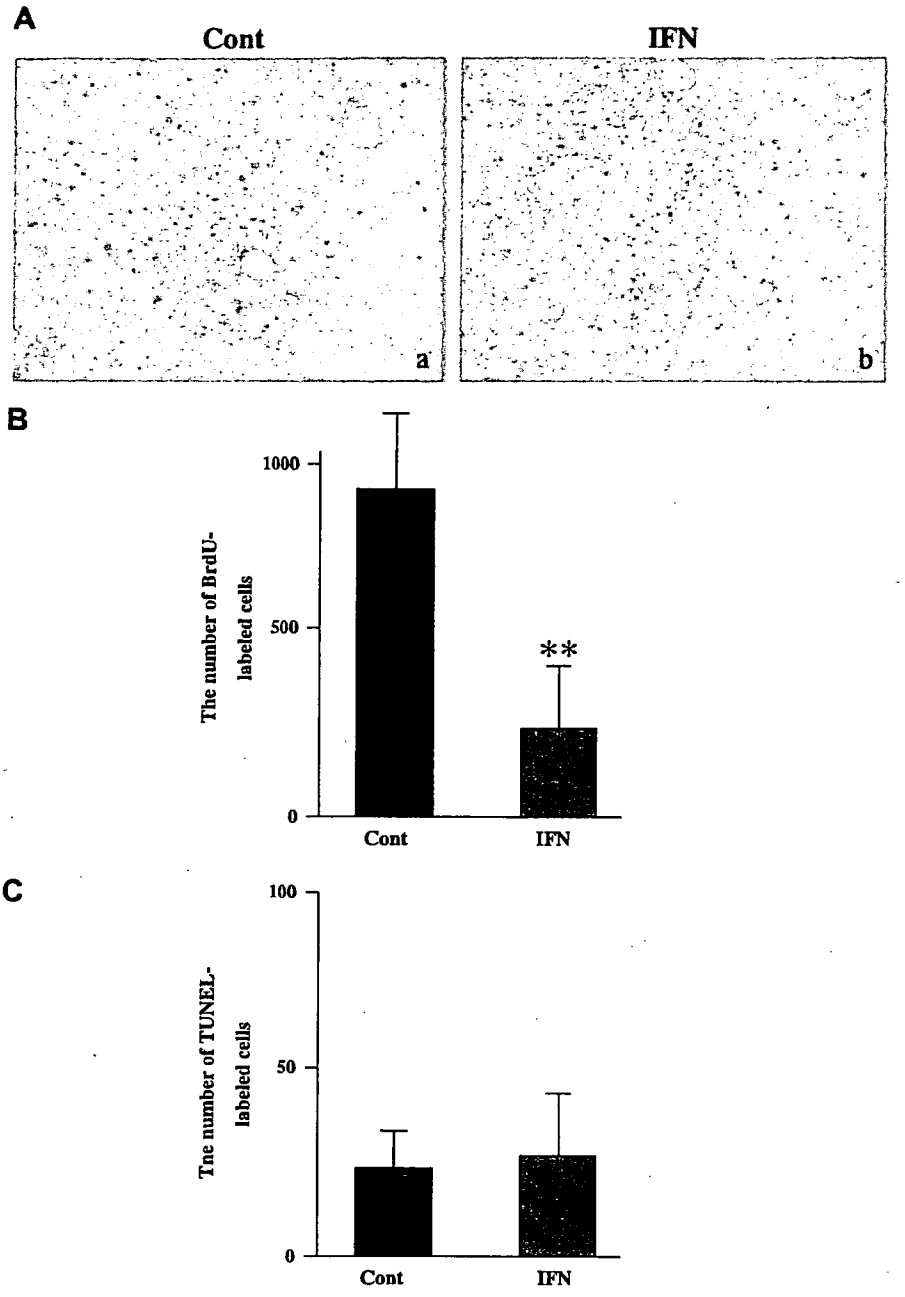

Fig. 2. (A) The results of immunostaining for BrdU in hepatocytes from HBx-Tg in *vivo*. HBx-Tg were treated with IFN-β or saline, and BrdU as described in Section 2. Paraffin-embedded liver sections were deparaffinized by three 5-min incubations in xylene, followed by several changes of ethanol (100%, 95%, 70% and 50%) and rehydration with water and phosphate buffered saline (PBS). Sections were immersed in methanol/3% hydrogen peroxide for 10 min to block endogenous peroxidase and then blocked by proper protein-blocker (supplied by the manufacturer). Slides were incubated with 1.5 M hydrochloric acid (HCl) before blocking of endogenous peroxidase and subjected to anti-BrdU (Dako, Japan). After counterstaining with hematoxylin, slides were dehydrated through graded alcohol, immersed in xylene and coverslipped. (B) BrdU-positive hepatocytes from three mice were counted throughout the whole slide at 400× magnification and the average number per mouse was obtained. The number of BrdU-positive cells is shown as means ± SD. IFN-β reduced the number of BrdU-positive cells significantly ($P < 0.01$). (Note that large stained spots consistent with nuclei of hepatocytes were counted and positively stained other cell types such as endothelial cells and Kupffer cells were not counted.) (C) The apoptosis-inducing effect of IFN-β on the HBx-Tg liver. The slides with the same sections used for BrdU staining were subjected to TUNEL analysis. Labeled cells were counted and statistically analyzed as for the BrdU staining. We could not see a significant increase in apoptotic cells following treatment with IFN-β.

IFN-β. In the experiment using primary culture lysates, HBx mRNA levels standardized by the expression level of mouse β-actin with or without IFN-β at 1 and 3 h were 0.410 ± 0.245 vs. 0.217 ± 0.115 ($P = 0.286$) at 1 h

and 0.183 ± 0.112 vs. 0.527 ± 0.480 ($P = 0.293$) at 3 h. The levels were 0.530 ± 0.016 vs. 0.501 ± 0.011 ($P = 0.682$) in the livers from HBx-Tg treated with or without IFN-β, respectively. Thus, there was no significant suppression by IFN-β of HBx mRNA either in the primary hepatocyte culture or in the liver tissues.

3.5. IFN-β specifically activates Stat 1 in mouse primary hepatocytes and WRL-68 cells

Western blot analysis was carried out to gain insight into the mechanism of inhibition of DNA synthesis in primary mouse hepatocytes and WRL-68 cells by IFN-β (Fig. 5A). Because Stat proteins are phosphorylated following the binding of type 1 IFN to the receptor, we tested for this phenomenon using specific antibodies. A significant induction of p-Stat 1 was observed in the primary hepatocytes and WRL-68 cells with 10,000 U IFN-β, compared to the levels of unphosphorylated Stat 1. In contrast to p-Stat 1, p-Stat 3 did not seem to be induced by IFN-β. A slight reduction of p-ERK (extracellular-signal-regulated kinase) was observed at 20 min after IFN-β treatment of the primary hepatocytes. We also compared the baseline levels of p-Stat 1 and p-Stat 3 without IFN-treatment between primary hepatocytes from HBx-Tg and those from wild-type mice (B). P-Stat 1 level was slightly higher in the wild-type mice than that of HBx-Tg. However, p-Stat 3 levels between those mice were not different.

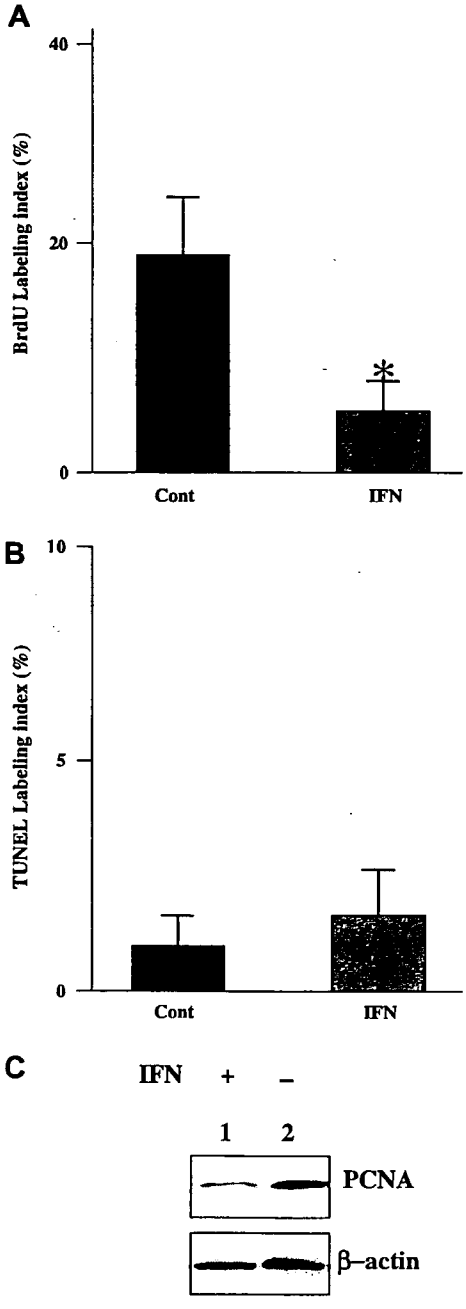

4. Discussion

We show herein that early treatment with IFN-β (for three months from 3 to 6 months of age) was sufficient to achieve significant prevention of HCC.

We confirmed that the administration of IFN-β suppressed DNA synthesis in the HBx-Tg liver, as well as in mouse primary hepatocytes derived from HBx-Tg mice (Figs. 2 and 3). A significant growth-inhibitory effect

Fig. 3. (A) The results of immunostaining for BrdU in primary hepatocyte derived from HBx-Tg. Hepatocyte viability was assessed using trypan blue exclusion and was between 85 and 90% in all experiments. Hepatocytes were seeded at 1.0×10^5 cells/ml in dishes coated with rat tail collagen (BD Bioscience, Japan) and cultured in William's E complete medium (Invitrogen, Japan) supplemented with 10% fetal calf serum (FCS), 0.5 μg/ml insulin (Sigma, Japan), for 2 h and then 20 ng/ml epidermal growth factor (EGF) (Sigma) with 10 mM nicotinamide (Sigma), and 30 μg/ml L-proline (Sigma) in 20 mM HEPES (pH 7.55) was added and the cells used experimentally. BrdU was added to the culture medium to 33 μM and incubated for 48 h with or without 1000 U/ml IFN-β. The cells were then fixed with cold absolute ethanol, incubated with 1.5 M HCl and subjected to a 1 in 200 dilution of mouse anti-BrdU antibody (Dako) at 4 °C overnight. They were then incubated with biotinylated anti-mouse IgG followed by the visualization with the Vectastain Elite ABC kit using diaminobenzidine as the substrate (Vector Laboratories, Burlingame, CA). Total labeled cells were counted in 40 fields (at 400× magnification). The labeling indices (percent of BrdU-positive cells) are shown as means ± SD. These were reduced significantly by treatment with IFN-β ($^*P < 0.05$). The results were confirmed by another two sets of experiments. (B) The apoptosis-inducing effect of IFN-β on primary hepatocytes. Primary mouse hepatocytes (1×10^5 cells/ml) obtained from HBx-Tg were seeded and incubated with or without 1000 U/ml IFN-β for 48 h and then fixed with cold absolute ethanol and subjected to TUNEL analysis. Labeled cells were counted and statistically analyzed as for the BrdU staining. We could not see a significant increase in apoptotic cells. (C) The level of expression of PCNA was suppressed by IFN-β treated for 24 h in the lysates obtained from primary hepatocytes of HBx-Tg by Western blot analysis.

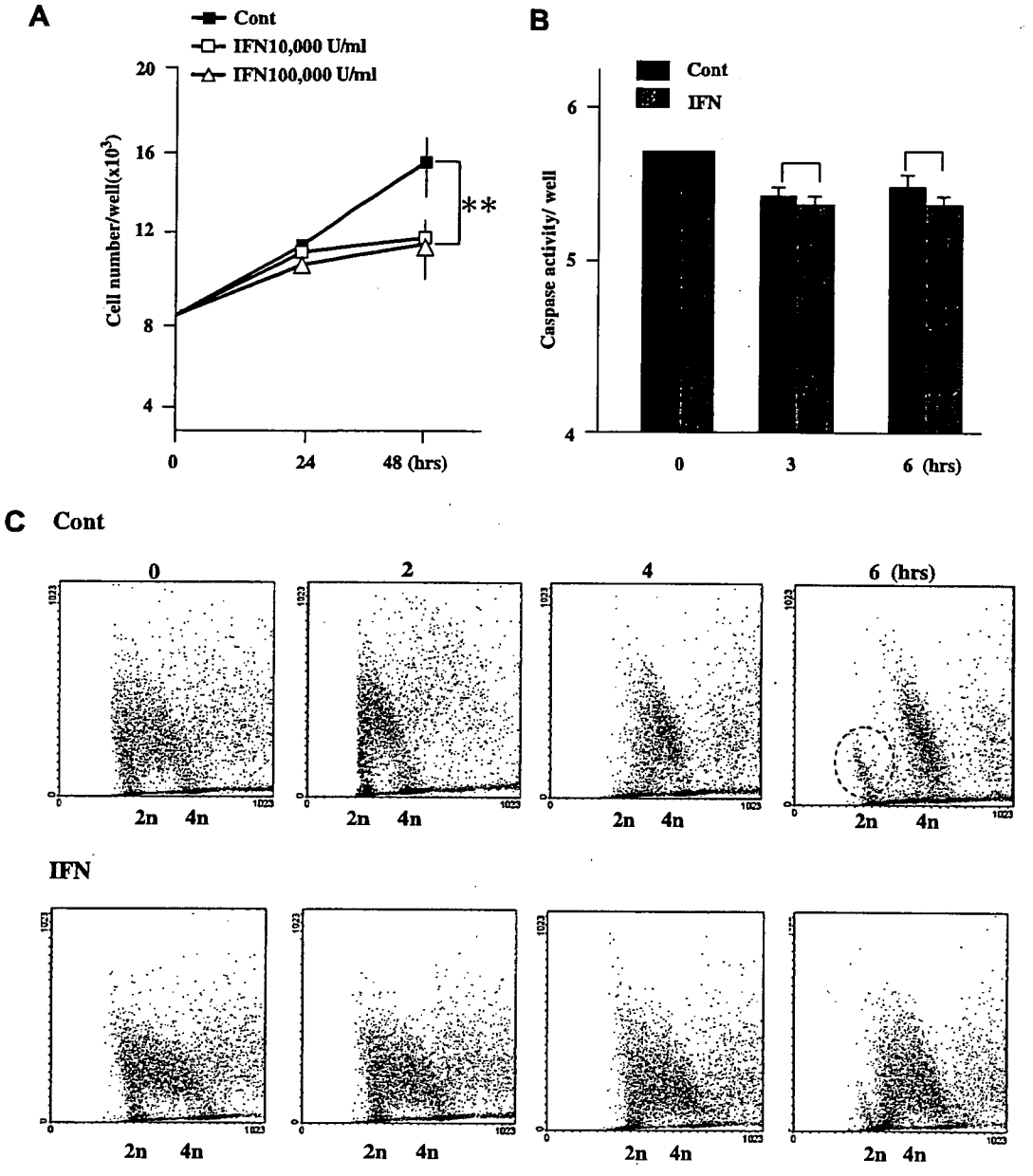

Fig. 4. (A). The growth-inhibitory effect of IFN-β on WRL-68 cells. A proliferation assay was performed by analyzing the number of viable cells using a modified MTT assay (Cell counting kit-8, Dojindo, Japan) according to the manufacturer's instructions. Cells (6.5×10^4 cells/ml) were seeded in triplicate in a 96-well microtiter plate, grown with 10% FCS for 7 h, and then fed with fresh medium including 10,000 or 100,000 U/ml IFN-β for 24 and 48 h. Ten microliters of a solution consisting of 5 mM WST-8 [2-(2-methoxy-4-nitrophenyl)-3-(4-nitrophenyl)-5-(2,4-disulfophenyl)-2H-tetrazolium, monosodium salt] was added and the cells incubated for 2 h. Cell numbers were estimated by measuring the absorbance with a microtiter plate reader (UltraspecVisible Plate Reader, Amersham-Pharmacia Biotech, Japan) by setting the test wavelength at 450 nm and the reference wavelength at 650 nm. Each experiment was repeated three times and analyzed statistically. IFN-β at 10,000 or 100,000 U reduced the number of viable cells significantly after 48 h ($^{**}P < 0.01$). (B) The apoptotic effect of IFN-β on these cells. WRL-68 cells (1×10^4 cells/ml) were incubated with 10,000 U/ml IFN-β for 3 or 6 h and assayed by a luminometer in triplicate, twice. An extremely high value was obtained by using purified caspase 3/7 (Sigma) as the positive control (data not shown). Statistical comparisons were made between the values at each time point. Data shown are means ± SD. We could not detect an increase of enzyme activity following IFN-β treatment for 3 or 6 h. (C) For cell cycle analysis, 10^6 cells were incubated with 10,000 U/ml of IFN-β or PBS for 24 h and labeled with 33 mM BrdU for 30 min. Cells were harvested and fixed each 2, 4, and 6 h after changing the medium to remove the BrdU. They were then treated for 20 min with 1.5 M HCl, incubated for 1 h with a 1 in 200 dilution of the mouse fluorescein isothiocyanate (FITC)-conjugated anti-BrdU antibody (BD Bioscience, Japan), stained with propidium iodide (PI) and analyzed by FACscan flow cytometer (Becton–Dickinson, Franklin Lakes, NJ). WRL-68 cells in the S phase (2 N) shifted gradually to the G2/M phase (4 N) and most of the cells were in this phase at 6 h, whilst a small population reappeared at G1 (upper panels, dotted circle). On the other hand, most of the IFN-β treated cells remained in the S phase, even at 6 h (lower panels).

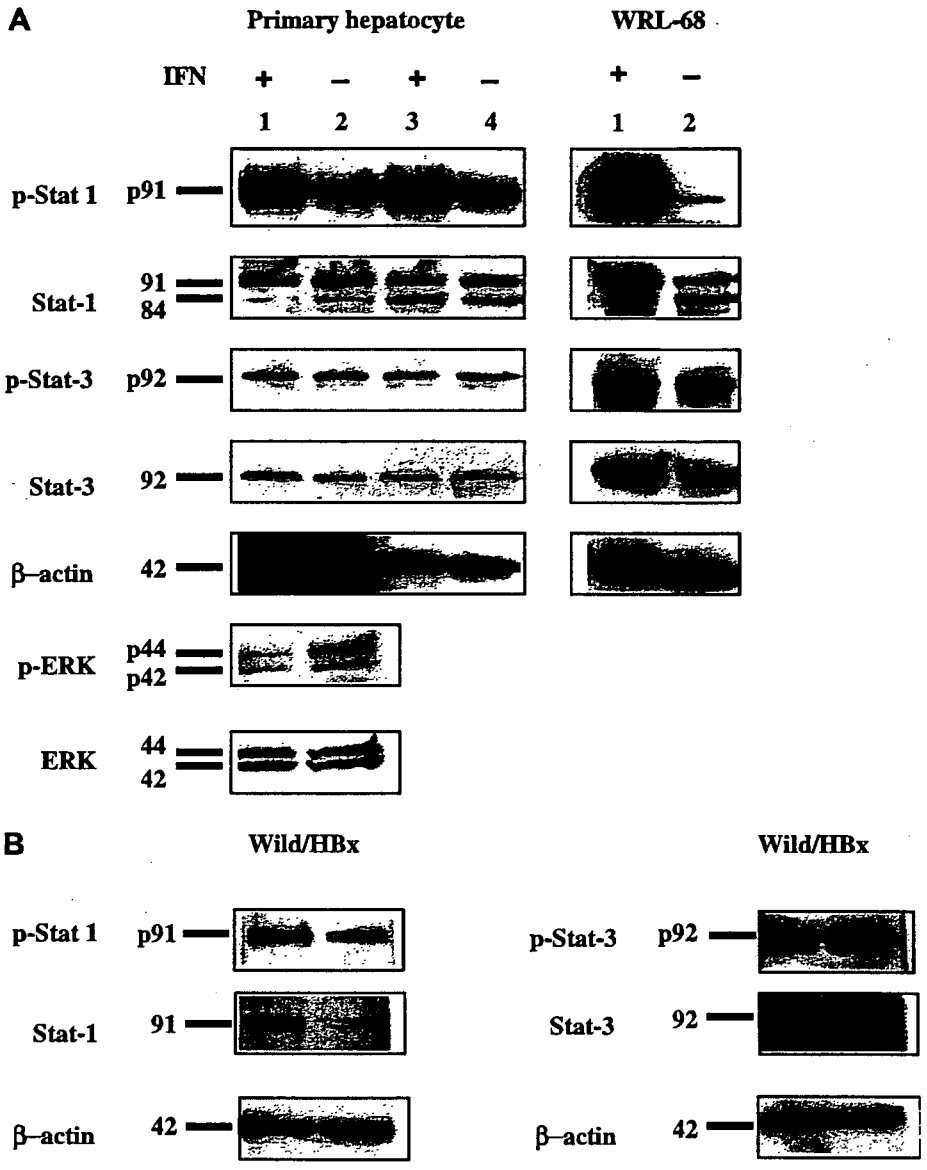

Fig. 5. Western blot analyses using cellular lysates obtained from primary hepatocyte culture derived from 6-week-old HBx-Tg (A, left) and WRL-68 cells (right) in the presence or absence of 10,000 U/ml IFN-β, and those from wild type (non-transgenic) mice and HBx-Tg (B). Proteins were isolated in ice cold lysis buffer (150 mM NaCl, 20 mM Tris/HCl [pH 7.8], 2 mM EDTA, 50 mM β-glycerophosphate, 0.5% TNP 40, 1% glycerol, 1 mM DTT, 10 mM NaF, 10 μg/ml leupeptin, 10 μg/ml aprotinin, and 2 mM phenylmethylsulfonyl fluoride). Laemmli buffer was added, the samples were boiled for 5 minutes, the aliquots were separated by SDS-PAGE, and subjected to Western blot analyses. (A, Left) The results of p-Stat 1, Stat 1, p-Stat 3, Stat 3, and mouse β-actin, p-ERK, and ERK in the mouse primary hepatocytes following treatment with IFN-β for 20 min (all) and 60 min (other than p-ERK and ERK). A significant increase of p-Stat 1 but not that of p-Stat 3 was observed following treatment with IFN-β. (Right) Because the cell-cycle block by IFN-β became apparent after 6 h treatment (Fig. 4C), we compared the effect of IFN-β after 24 h incubation of WRL-68 cells. The results of p-Stat 1, Stat 1, p-Stat 3, Stat 3, and β-actin, by the treatment of IFN-β, are shown. A significant increase of p-Stat 1 but not of p-Stat 3 was also observed following treatment with IFN-β. (B) The results of p-Stat 1, Stat 1, p-Stat 3, Stat 3, and mouse β-actin in the lysates from wild and HBx-Tg. A baseline level of expression of p-Stat 1 and p-Stat 3 in the primary culture was detectable in the before adding IFN-β and this was probably due to the effect of EGF in the medium on the activation of Stat proteins [40,45,46]. The level of p-Stat 1 in the wild type mouse was slightly higher than that of HBx-Tg. In contrast, the levels of p-Stat 3 did not differ between them.

also was observed in the WRL-68 cell line and was attributable to the effect of IFN-β on the cell cycle, with blockade at S phase (Fig. 4A and C). From these observations, the main mechanism of the antiproliferative effect of IFN-β that may result in the inhibition of hepatocarcinogenesis in our mouse model may be attributable to the block of DNA synthesis and cell cycling. Interestingly, although the treatment with IFN-β was temporal, the number of hepatocytes with DNA synthesis remained lower 3 and 12 months later in life

(Fig. 1D). The inhibition of DNA synthesis and block of cell cycling seem to have a remote effect in suppressing the proliferation of hepatocytes and improving the cancer-prone tendency of the liver. The precise mechanisms of this phenomenon are unknown. However, at least the inhibition of DNA synthesis by treatment with IFN-β may reduce the chances of acquisition of genetic abnormalities, contributing to the delay of hepatocarcinogenesis in these mice.

In our model, the HBx gene is the main factor involved in transforming hepatocytes [24]. Suppression of HBx gene expression may be the most likely mechanism to explain the inhibition of HCC, which is a similar scenario to the previous experiments using c-myc transgenic mice, where repression of c-myc was the main cause of the reduction of cell proliferation [27,28]. In contrast, we could not see significant suppression of HBx gene expression by IFN-β, although we could see significant inhibition of DNA synthesis in vitro and in vivo. A possible explanation of this difference may be that IFN-β inhibited some downstream events originating from HBx action, which eventually are associated with the inhibition of DNA synthesis.

In this study, we shed light on the preventive effect of IFN from the aspect of inhibition of DNA synthesis and cell cycling. So far, animal models of hepatocarcinogenesis for which IFN has been reported to be beneficial were based on an oncogenic transgene [27,28], including this study, or induced by chemicals [29], and not influenced by inflammation. Thus, the rationale for prevention of HCC shown in this study may be applicable to these models. Furthermore, it can also be extrapolated to human hepatocarcinogenesis that in general occurs by the continuous regeneration of hepatocytes due to necroinflammation caused by factors such as chronic viral infections.

The mechanisms by which IFN-β exerted its antiproliferative effect are intriguing. Stat 1 seems to exert primarily antiproliferative effects [40,41] and Stat 3 may have pro-mitogenic and anti-apoptotic effects [42,43]. Phosphorylation of Stat 1 was significantly enhanced by IFN-β in mouse primary hepatocytes and WRL-68 cells. In contrast, we could not observe an increase in phosphorylation of Stat 3 in either cell type. The enhanced expression of p-Stat 1, but not that of p-Stat 3, might be associated with the inhibition of DNA synthesis and reduction of PCNA expression in the primary hepatocytes. In addition, the level of p-Stat 1 was slightly higher in the primary hepatocytes from wild type mice than that from HBx-Tg (Fig. 5B). This result confirms that the restoration of p-Stat 1 levels by IFN contributes to the prevention of HCC development in HBx-Tg.

A recent study using a HCC cell line showed that IFN-α induced antiproliferative signaling via the Stat 1 pathway and reduced the growth stimulation signaling by cross talk with MEK/ERK pathway [44]. In our study, a slight reduction of phosphorylated ERK following IFN-β treatment also was observed in the primary hepatocytes. This indicates the possible involvement of the MEK/ERK pathway, initiated by the induction of p-Stat 1, in the inhibition DNA synthesis in the hepatocyte. Future analysis may clarify the signal pathways through the activation of Stat 1 to the inhibition of DNA replication, elucidating the molecular mechanisms of antiproliferative function of IFN-β that contribute to the prevention of hepatocarcinogenesis.

Acknowledgement

We are grateful to Dr. Minoru Nomoto (Niigata University) for the histological diagnosis and evaluation of the mouse tissues.

References

[1] Okuda K. Hepatocellular carcinoma: recent progress. Hepatology 1992;15:948–963.
[2] Feitelson MA, Sun B, Satiroglu Tufan NL, Liu J, Pan J, Lian Z. Genetic mechanisms of hepatocarcinogenesis. Oncogene 2002;21:2593–2604.
[3] Farazi PA, Depinho RA. Hepatocellular carcinoma pathogenesis: from genes to environment. Nat Rev Cancer 2006;6:674–687.
[4] Yu MC, Yuan JM. Environmental factors and risk for hepatocellular carcinoma. Gastroenterology 2004;127 (Suppl. 1):S72–S78.
[5] Shiratori Y, Moriyama M, Arakawa Y, Ide T, Sata M, Yoshida H, et al. Interferon therapy reduces the risk for hepatocellular carcinoma: national surveillance program of cirrhotic and noncirrhotic patients with chronic hepatitis C in Japan. Ann Int Med 1999;131:174–181.
[6] Takimoto M, Ohkoshi S, Ichida T, Takeda Y, Nomoto M, Asakura H, et al. Interferon inhibits progression of liver fibrosis and reduces the risk of hepatocarcinogenesis in patients with chronic hepatitis C: a retrospective multicenter analysis of 652 patients. Dig Dis Sci 2002;47:170–176.
[7] Imai Y, Kawata S, Tamura S, Yabuuchi I, Noda S, Inada M, et al. Relation of interferon therapy and hepatocellular carcinoma in patients with chronic hepatitis C. Osaka hepatocellular carcinoma prevention study group. Ann Int Med 1998;129:94–99.
[8] Shiratori Y, Ito Y, Yokosuka O, Imazeki F, Nakata R, Tanaka N, et al. Antiviral therapy for cirrhotic hepatitis C: association with reduced hepatocellular carcinoma development and improved survival. Ann Int Med 2005;142:105–114.
[9] Ikeda K, Saitoh S, Suzuki Y, Kobayashi M, Tsubota A, Fukuda M, et al. Interferon decreases hepatocellular carcinogenesis in patients with cirrhosis caused by the hepatitis B virus: a pilot study. Cancer 1998;82:827–835.
[10] Soga K, Shibasaki K, Aoyagi Y. Effect of interferon on incidence of hepatocellular carcinoma in patients with chronic hepatitis C. Hepatogastroenterology 2005;52:1154–1158.
[11] Stark GR, Kerr IM, Williams BR, Silverman RH, Schreiber RD. How cells respond to interferons. Annu Rev Biochem 1998;67:227–264.
[12] Platanias LC. Mechanisms of type-I- and type-II-interferon-mediated signalling. Nat Rev Immunol 2005;5:375–386.
[13] Yano H, Iemura A, Haramaki M, Ogasawara S, Takayama A, Akiba J, et al. Interferon alfa receptor expression and growth inhibition by interferon alfa in human liver cancer cell lines. Hepatology 1999;29:1708–1717.